Effect of Stress Distribution in Designing Reverse Shoulder Prosthesis: A Finite Element Analysis

Samaneh Aghazadeh

Submitted to the
Institute of Graduate Studies and Research
in partial fulfillment of the requirements for the degree of

Master of Science
in
Mechanical Engineering

Eastern Mediterranean University
September 2015
Gazimağusa, North Cyprus

Approval of the Institute of Graduate Studies and Research

Prof. Dr. Serhan Çiftçioğlu
Acting Director

I certify that this thesis satisfies the requirements as a thesis for the degree of Master of Science in Mechanical Engineering.

Prof. Dr. Uğur Atikol
Chair, Department of Mechanical Engineering

We certify that we have read this thesis and that in our opinion it is fully adequate in scope and quality as a thesis for the degree of Master of Science in Mechanical Engineering.

Asst. Prof. Dr. Neriman Özada
Supervisor

Examining Committee

1. Assoc. Prof. Dr. Hasan Hacışevki

2. Asst. Prof. Dr. Neriman Özada

3. Asst. Prof. Dr. Mostafa Ranjbar

ABSTRACT

One of the extreme diseases among patients are Rotator cuff tear and degenerative shoulder join, which result in stark pain and shrink performance in shoulder joint. Nowadays, a substitute shoulder is the best way to relieve pain and reestablish stability. A reversed spare shoulder is needed whenever, the substitute shoulder isn't efficient enough to refurbish the joint. The only difference between those two components is that the reverse replacement is similar to the normal shoulders. For instance, the ball component is positioned to the glenoid and the socket is placed to the proximal humerus. The main reason of the altered anatomy is to provide a greater lever arm for the deltoid muscle to regain active shoulder elevation. Identically to other inventions, reversed replacement has inconvenient, such as loosening in glenohumeral joint and failure of prosthesis at the glenoid attachment area.

The main purpose of this thesis is to recognize the probable failures at any of the implant`s components like the glenoid and glenohumeral joint. 3D model of reverse shoulder implant was created using the software SolidWorks in order to perform finite element analysis (FEA). The finite element (FE) analysis has been carried out in this study via ANSYS software to obtain the maximum values for Von Mises stress on each component, in order to evaluate the values and see if the designed component would sustain during the three analyzed movements (abduction, flexion and rotation) for a movement span of 4 seconds. It is hypothesized that the range of motion (ROM) of the shoulder joint is altered with reverse shoulder implant. An investigation is carried out concerning the extent of contact stress to cause wear of the humeral cup in glenohumeral joint.

The results show that the maximum stress of the polyethylene made humeral cup happens during abduction, and it can get as high as 26 MPa that exceeds the polyethylene yield strength. This high value of stress Polyethylene would probably wear which can lead to joint loosening of reverse glenohumeral joint. Also according to the obtained results the two screws used in the implementation of the implant (Inferior screw and Superior screw) are the componets with the maximum Von Mises Stress, especially in flexion movement (maximum stress of 134 MPa for superior screw). Almost in all three movements these screws are the most critical component however their maximum stress does not become critical since it does not exceed 15% of the titanium yield strength (neither compressive or tensile). Hence the titanium alloy parts of the implant would not become critical for the design.

On an overall conclusion the results shows that in the design of humeral cup, the abduction movement is the key movement since it has the most stress impact on this component, and similarly the flexion movement is the key movement in the design of the baseplate and connection screws.

Keywords: Shoulder arthroplasty, Finite Element, Shoulder 3D modeling, Von Mises stress equivalent

ÖZ

Omuz ağrılarına ve omuz hareketlerinin engellenmesine sebep olan en önemli rahatsızlıklardan biri “Rotator Cuff” yırtılmasıdır. Omuzdaki ağrıları dindirmek ve omuz ekleminin dengesini sağlamak için kullanılan bazı yöntemler vardır. Fakat, birçok tedavinin sonuç vermemesi sebebi ile omuz eklemini tedavi etmek için ters eklem protezine ihtiyaç vardır. Ters omuz protezi de düz omuz protezine benzer şekilde üretilir fakat yalnızca küre kısmı ile oyuk kısım yer değiştirmiş şekildedir. Normal omuz protezinde küre kısmı kol kemiği ve oyuk kısım da kürek kemiği yerine monte edilir. Bunun tam tersi olarak, ters omuz eklemi protezinde küre kısmı kürek kemiği üzerine ve oyuk kısım ise kol kemiği üzerine monte edilmektedir. Ters omuz eklemi protezinin kullanılmasının en büyük amacı omuzu saran delta şeklindeki “Deltoid” kasının kolu kaldırma hareketinde daha aktif rol oynayabilmesidir. Fakat, ters omuz protezinin avantajlarının yanında protezin kaybı ve protez parçalarının kırılması gibi önemli dezavantajlar da görülebilmektedir.

Bu tez için yapılan çalışmanın amacı, ters omuz protezinde bulunan kol kemiği ve kürek kemiği arasındaki eklemin ve protez parçalarının kırılma olasılıklarını bulabilmektir. Öncelikle SolidWorks yazılımı kullanılarak üç boyutlu ters omuz protezi modeli oluşturuldu. Daha sonra bu model sonlu elemanlar analizi gerçekleştirmek için ANSYS yazılımına aktarıldı. Ters omuz protezinde bulunan tüm parçalar ile kürek kemiği ve kol kemiğinin de Von Mises stres analizleri yapılıp stres yoğunluğunun dağılımları da incelendi. Protez parçalarının stres analizi kolun üç farklı hareketi altında incelenip, harekete bağlı olarak da stres dağılımları bulundu. Bu sonuçlar ters omuz protezi parçalarının tasarımında değişiklik yapılıp yapılmaması

gerektiği konusunda da bizi aydınlatmıştır. Bu çalışmada omuz hareketlerinin parçalar üzerindeki stres dağılımında etkili olabileceği hipotezi ortaya konuldu ve doğruluk payı kanıtlandı. Bunların yanında omuz eklemi arasındaki kontak stres de incelenerek aşınmaya sebep olup olmadığı da bulundu.

Elde edilen sonuçlar, UHMWPE kullanılarak üretilen "humeral cup" parçasında oluşan stresin en yüksek değerinin 26 MPa olup "abduction" hareketinde görüldüğü tespit edilmiştir. Bu stress değeri UHMWPE maddesinin mukavemet değerinden daha yüksek olduğu görülmüştür. Bu sonuç, ters eklem protezi takılan kişinin abduction hareketi sırasında "humeral cup" üzerinde oluşan stresin aşınmaya ve protezin kaybına yol açabileceği bulunmuştur. Incelenen diğer hareket olan flexion hareketindeyse, "Inferior screw" ve "Superior screw" parçalarının en yüksek stress altında oldukları bulunmuştur. Incelenen tüm omuz hareketleri içinde en kritik ve kırılmaya eğilimli parçaların da "Inferior screw" ve "Superior screw" oldukları belirlenmiştir. Son olarak, yapılan bu çalışmada, en kritik hareketlerin "abduction" ve "flexion" olduğu ve sırasıyla "humeral cup" ile baseplate ve "Inferior screw" ve "Superior screw" parçalarının kırılmasına neden olabileceği belirlenmiştir.

Anahtar Sözcükler: Ters omuz artroplastisi, sonlu elemanlar, omuz modeli, Von Mises stres

ACKNOWLEDGMENT

I would like to thank to my supervisor Assist. Prof. Dr. Neriman Ozada for her support, remarks and comments through writing my master thesis.

I also would like to thank my family for their invaluable support and encouragement during my studies. I also would like to thank Ramin Layeghi for his moral support and guidance. Also I would like to point out that all the rights of this reverse shoulder implant, Verso® belongs to its manufacturer BIOMET Company, and I would like to express my gratitude for providing us the implant information.

TABLE OF CONTENTS

LIST OF TABLES

LIST OF FIGURES

LIST OF ABBREVIATIONS

3D	Three Dimensional
CT	Computed Tomography
DOF	Degree of Freedom
FE	Finite Element
FEA	Finite Element Analysis
FEM	Finite Element Modeling
MRI	Magnetic Resonance Imaging
Pa	Pascal
ROM	Range of Motion

Chapter 1

INTRODUCTION

1.1 Foreword

Due to the high degrees of freedom (DOF) of the shoulder girdle, its joints are prone to injury as well as affected by diseases like arthritis. Therefore the shoulder joints have long been investigated biomechanically to understand the normal and abnormal joint functions for better treatments. The rotator cuff tears of glenohumeral joint which is the main joint of the shoulder girdle, have been treated by joint replacement surgery with applying reverse shoulder implants. In order to understand the function and failure possibilities of the reverse shoulder implants, biomechanical studies are required to improve the implant design and reduce the rate of the failures. In this study, it is aimed to provide wide range of information about the mechanics of anatomic and implanted shoulder joint with the analysis of implant failure.

1.2 Main Joints and Bones of Shoulder Girdle

The glenohumeral joint is one of the important joints in the human body allowing a wide range of motion to be able to position the upper arm and lower arm. Glenohumeral joint is also prone to dislocation and instability due to its high range of motion.The three main bones of the shoulder girdle are the humerus, clavicle, and scapula. The brief explanation about these bones is provided as follows.

1.2.1 Humerus

The main and longest bone in the upper part of our body with a greater margin is called the humerus. The humerus is the largest bone of the upper extremity, its proximal

portion includes the head and groove, lesser tuberosity and proximal humeral shaft. The humeral shaft angle at the anatomical neck is approximately between 130 degree and 150 degree which is important information for the replacement surgery [1].

1.2.2 Scapula

The bone lying on the posterolateral features of the thorax overlying ribs 2 from the first to the last 7 is called scapula [2]. It is served as a site of muscle attachment from thorax to shoulder girdle. Most important parts of the scapula are acromion, coracoid and glenoid. The acromion serves as a lever arm to function the deltoids, and forming the acromioclavicular joint. The roof of the rotator cuff is also formed by the acromion. Moreover, scapula provides the bony foundation for the normal range of shoulder joint [3].

1.2.3 Clavicle

The clavicle is only the sole strut bone which is connected to the shoulder girdle through sternoclavicular joint in the middle and by acromioclavicular joint laterally. There is a double curve along its long axis and it is subcutaneous in full extent. For muscle and ligaments, the flat outer third serves as on attachment point, whereas axial loading is accepted by tubular medial third. The weakest and thinnest portion is the middle third transition zone where most fractures accrue is this area [4]. The clavicle is important for muscle attachments, it also protects neurovascular structures and it supports the shoulder complex to protect it from displacing medially with activation of pectoralis and other axiohum−articular cartilage of humeral head. Additionally, the clavical stops inferior shifting of shoulder girdle through coracocla−viscular ligaments [5].

1.3 Musculoskeletal Joint Articulation

The most important shoulder joints are glenohumeral joint, acromioclavicular joint and sternoclavicular joint. These joints are briefly described in the following sections.

1.3.1 Glenohumeral Joint

The glenohumeral joint is between the humerus and glenoid which possesses great degree of mobility. Only 25 % or 30 % of the humeral head is in touch with glenoid during the joint movement [6]. This joint is assumed and modelled to be a three DOF ball and socket joint, and there are abduction-adduction, internal-external rotation, flexion-extension rotations of the glenohumeral joint. Interaction of stationary and active (muscle) forces consequence accurate resistance of the center of rotation through a large motion arc of shoulder. Muscle powers overstress and improving the result of the articular planes, and near the glenoid center direct concavity-compression effect is produced [7].

1.3.1 Acromioclavicular (AC) joint

Between the bones clavicle and the medial border of the acromion there is a joint called the acromioclavicular joint. This joint is completely enclosed by a capsule and its average size is 9 × 19 mm [8]. Nervous tension on the articular plane is high and can cause a breakdown or problem like osteolysis in weight lifters or osteoarthritis due to high axial loads relocated through its small surface area. Static stabilizers are composed of capsule, intra-articular disc, and ligaments that supply constancy to the acromioclavicular joint. This joint is covered by the capsule, which is thicker superiorly and anteriorly. Through the acromioclavicular ligaments superiorly, inferiorly, posteriorly, and anteriorly it is made unbreakable [9].

The superior acromioclavicular ligament has strings which are bent among the fibers

of the deltoid and trapezius muscles and they are strongest fibers. The coracoclavicular ligaments supply constancy of the acromioclavicular joint, which serve as the major suspensory ligaments of the upper boundary. The shoulder girdle is balanced by these ligaments at a regular distance. Acromioclavicular ligaments act as the main controller of the AC joint at which the coracoclavicular ligaments act as the main controller for vertical dislocation [10]. The common AC separation injury corresponds to progressions of the level of injury, first to the acromioclavicular joint and then secondly the coracoclavicular ligaments.

Sternoclavicular Joint:

Between the upper edge and the axial skeleton the joint that performs the actual articulation is the sternoclavicular joint. This joint is formed by the upper portion of the sternum and the articulation of medial end of clavicle also known as a saddle joint [11]. Given the great disparity in size between the large bulbous end of the clavicle and the smaller articular surface of the sternum, stability is provided by the surrounding ligamentous structures. From the connection of the first rib, the intra-articular disc-ligament composition begins which passes through the sternoclavicular joint, and attaching to the superior and medial clavicle this structure is a dense and fibrous. To check the middle dislocation of the inner clavicle this disc-ligament is playing very important and central role [7].

To join the lower surface of middle clavicle the costoclavicular ligament attaches the upper surface of the first rib. The frontal fibers oppose extreme upward rotation and the posterior fibers oppose extreme downward rotation are revealed by bearnmo experiment. The superomedial portion of clavicle is connected to capsular ligaments and upper sternum by the interclavicular ligament to test extreme downward rotation

of clavicle. The anterosuperior and following features of the sternoclavicular joint are covered by capsular ligament [12]. The anterior portion acts as main preservative against upward displacement of the inner clavicle and is intense and stronger than the posterior portion and a sliding force on the distal ending of the shoulder roots. 30 degree to 350 degree of upward increase, 350 degree of forward and backward motion and 450 degree to 500 degree of axis rotation can be done by sternoclavicular joint [4].

1.4 Shoulder Joint Muscle Functions

Shoulder muscles play important role to stabilize the shoulder joint such as rotator cuff muscles. Rotator cuff muscles are the most functional muscles of the upper extremity.

1.4.1 Rotator Cuff Muscles

The rotator cuff is a group of muscles. This group comprises of the subscapularis, supraspinatus, in-fraspinatus, and teres minor. They perform a forceful steering mechanism. Dynamic relation among the muscles comprising the rotator cuff and the fixed stabilizers creates the three-dimensional activities or rotations of the humeral head. Rotary motion and depression in positions of abduction in the humeral head is because of rotator cuffs activation [13]. As compared to the large external muscles such as the deltoid, pectoralis major, latissimus dorsi, and trapezius, the rotator cuff muscles are smaller in cross-sectional area and size because they lie much closer to the center of rotation on which they act. To provide stability and improvability to a dynamic fulcrum all through glenohumeral abduction, the rotator cuff is very well positioned according to its anatomical location [14].

1.4.1.1 Subscapularis

The anterior portion of the rotator cuff is included in the subscapularis muscle. On the smaller tuberosity of the humerus to enlarge across to its placing it begins from the

subscapular fossa. With the anterior capsule the muscle of the subscapularis is systematically connected. Along the inferior border of the scapula the auxiliary nerve passes and as a result subject to disorder from frontal dislocation. Especially in maximum interior rotation the subscapularis acts as an internal rotator, innervation is from the upper and lower subscapular nerves [4].

1.4.1.2 Supraspinatus muscles

The supraspinatus muscle at the superior of the greater tuberosity of the humerus is originated from the supraspinatus fossa. It is operated for the abduction and elevation movement of shoulder joint. Moreover, it stabilizes the glenohumeral joint and provides external rotation force.

1.4.1.3 Infraspinatus muscle

The infraspinatus gets enlarged across from the infraspinous fossa and make bigger across to its tendinous placing on the middle face of the greater tuberosity [10]. The primary external rotation force is provided by the infraspinatus, alongside with the teres negligible; also adjacent to posterior subluxation, it stabilizes the glenohumeral joint. Innervation is from the suprascapular nerve.

1.4.1.4 Teres minor

The teres minor originates from the mid to upper regions of the axillary border of the scapula and extends laterally and superiorly to its insertion on the most inferior facet of the greater tuberosity. In concert with the infraspinatus, the teres minor is an external rotator and glenohumeral stabilizer. Innervation is from the axillary nerve [14].

1.5 Organization of the Thesis

This thesis includes six chapters, the Appendix and References. Functional anatomy of normal shoulder, which includes important bony parts and muscles around them, joint movements, and biomechanical information are explained in Chapter1. In

Chapter 2 Literature Survey is conducted and the previously published biomechanical models of the shoulder joint, state of the art about the shoulder implant failure, implant components and complications of the shoulder replacement are presented. Design steps of reverse shoulder joint implant components and the FE modelling are provided in Chapter 3. The results are demonstrated in Chapter 4 and discussed in Chapter 5. Finally, the conclusion and suggestions for future work are presented in Chapter 6.

Chapter 2

LITERATURE REVIEW

2.1 State of the Art in the Modeling of Shoulder Joints

In the field of orthopedics, the biomechanical modeling is getting important which can provide us the biomechanical information about the anatomic and artificial joints, stress and strain changes, failure mechanisms and material behavior.

Considering the shoulder joint prosthesis, having a previse sample can be helpful for surgeons to overcome some problems occur during or after the replacement surgery and to guide proposing appropriate type, size and position of the shoulder prosthesis. FE models are being utilized in medical research which has ability to fully analyze complex models which are difficult to be studied experimentally [15]. For example, FE methods have been used to enhance a numerical sample of the shoulder to see effect of humeral head's shape on stress distribution in the scapula. This method has long been used to compare normal and artificial shoulder joints, to identify the reason of failure or complications.

It is understood from many researches that changed geometry of the pathological shoulder can be another factor of posterior subluxation for osteoarthritic shoulder in clinical circumstance like rigidification and subscapularis muscle as often postulated.

On the other hand in another study, Madymo® [16], which is mathematical dynamic modeling software package progressed by Tno® [16], were used to dissect 3D forces and torques at shoulder joint during movement. Something like 40 years old man with healthy shoulder participated without any previous shoulder joint disease, injury or disability. Needed data like weight, height and length of the right upper limb segment were gained. For analyzing forces and torques, gained shoulder joint spaces and angles by a simple program were used as input data for the computer sample to make a simulation of the subject's movements. Two possible situations were, being stable in nature being comfortable and moving correctly in abduction and flexion up to 90 degree departed, extension and mixture of and adduction movements. Second situation acts as the same in steps but there's a difference that having a 2.5 kg. Weight held in the right hand. At the end shoulder joint force and torque were successfully predictable [16].

Some mechanical solicitation in Humerus is gained in survey by analyzing glenohumeral joint during external and internal rotation for an ordinary humerus. FE method was used with utilizing the ANSYS software. All muscles and shoulder movements were modelled and correlated as Deltoidus and brahialisnas muscles whiting internal rotation, Infraspinatus, Trese minor, Deltoidus and Supraspinatus were participating in external rotation movement. 22N force that was a different assumption in the study was applied in every individual insertion point on humerus. The same mechanical stress, the same strain and the whole deformation were thought to be for both internal and external rotation of shoulder as the main consequence of the survey. Proximal epiphysis was known as the highest amount of strain region in both shoulders, but it was placed close to the prosthesis head in un-prosthesis shoulder meanwhile it was placed humeral head for an ordinary shoulder. The same stress

distribution for both shoulder had the same result. The highest amount of stress was seen in to the close epiphysis on the humeral head for ordinary shoulder and close to the head at joint portion between bone and prosthesis for the prosthetic shoulder. In the same humeral region of internal rotation the highest amount of deformation didn't accrue, but it was place at the middle of diaphysis and under the middle of the diaphysis. A bit closer to the distal humerus for the ordinary one, respectively [17].

2.2 Need for Shoulder Joint Replacement

Patients have different complications to be considered for a shoulder joint replacement because of having different shoulder problems. Rotator cuff tear, osteoarthritis and fractures are the most common reasons for the replacement. The main action of rotator cuff is to keep glenohumeral joint stable and attach the humerus to the scapula. The rotator cuff tendons are not totally attached to the humerus, when one or more of tendons are torn, it influences the movement of the joint. This causes some problems like Subacromial Impingement, instability of humeral head. These problems might be caused by proximal movement of humeral head where the bursa can be inflamed [18] [19]. Shoulder joints can be replaced because of arthritis, osteoarthritis that are the most common diseases among millions of people around the world [20]. The reason of these diseases are not fully understood which also involved in some sport activities. Fractures can be known as the main cause of replacement for shoulders [20] [21]. For shoulder joints, totally, the fracture girdles are divided in three parts which are proximal humerus, clavicle and scapular fractures. Scapular fracture happens less common than the other types of fracture which is about 5% of them. It is mostly common among females more than 60 years old and osteoporotic patients. 85 % of this type of fracture is not displayed and it's not necessary to be operated [22].

In a close classification the proximal humerus is made of four parts that are humeral head, greater tubercle, lesser tubercle and humeral shaft. 1 cm moving of fracture fragments and 45º or more change in the angle is considered as separated part for fragments. Clavicle fracture is often happens due to direct effect. As one example in contact sports and it is more frequent among adults younger than 30 years old. 80 % of this fracture is in lateral one-fifth of clavicle. Scapula fracture in the shoulder girdle is not common because of existence of muscle coverage around it that's why this type is only 0.3 % of all types, and the main reason of this type of fracture is direct trauma. Therefore, modelling and understanding the mechanism of injuries, fractures and abnormal joint functions can yield us to design implants to treat these problems more effectively and improve the orthopaedic technologies [22].

2.2.1 Treatment Methods of Shoulder Joint Problems

Totally, there are two types of treatments as surgical and nonsurgical. Patient's condition determines the type of treatment. Even selecting nonsurgical type treatment it depends on pain level and also intensity of disease of the patient. One of the nonsurgical types of treatment is common for osteoarthritis is physiotherapy, activities like swimming and using nonsteroidal anti-inflammatory drugs. Related exercises to Range of motion joint movement process could be effective to tranquil pain and enhance motion and also glenohumeral joint injections like steroid and hyaluronan are examples of suggestion for patient who are unable to cope with exercises [23]. On the other hand for some fractures like humeral neck and scapular body surgery is not a good solution, instated we can immobilize the shoulder and local ice for healing fractures after a period of time we can gently mobilizing the part can be helpful. In addition some handy therapies like message, dry needling and electrotherapy can support the healing process [24]. As the last solution when nonsurgical treatment

doesn’t appear to work, some surgeons suggest surgical treatment like reduction internal fixation or total joint replacement [25] [26].

2.2.2 Repeated Replacement Surgeries of Shoulder Joint

Shoulder joint replacement and also arthroplasty is increasing, so that the amount of revision surgery is increasing as well. Artificial shoulder joint problems are component malposition, infection, fracture and instability of joint after primary arthroplasty that compels surgeons to decide that revision surgery could be a solution [27]. Unconstrained implants, fusion or resection arthroplasty are superior to reverse shoulder arthroplasty [28]. In a survey, loss of forward flexion and outer rotation after revision shoulder arthroplasty using an unconstrained prosthesis were absorbed. In another research [29], patients who underwent revision arthroplasty that used hemiarthroplasty method with weak bone stock on the glenoid were observed and studied. Comparing with the samples that had enough bone stock on the glenoid and entire shoulder arthroplasty were operated for them. There were even weaker result and also the complication rate was high [29].

In a survey 28 patients (about 30 shoulders) who were 16 females and 12 males were followed up for minimum 24 months patients underwent revision operation revers. Shoulder arthroplasty between 2005 and 2008 by the same surgeon in the same instate because of unsuccessful prior shoulder arthroplasty. The study included 11 shoulders were revised from an unsuccessful humeral head arthroplasty. Revision operation was considered for about 21 right and 9 left shoulders. The age range was between 43 to 81 years (mean age of 64 years) classic osteoarthritis in 33 % which is connected with fracture in 30 %, cuff tear arthroplasty in 13 % capulorrhaphy arthroplasty in 17 % and avascular in 7 % were observed as index operation. In addition, more than a shoulder arthroplasty had a surgery in 17 shoulders and 13 shoulders had only one arthroplasty

just before revision operation. Strength to forward lifting and range of motion, which was accessed in active forward flexion, abduction and outer rotation. As a consequence a developing progress was observed in all categories except in active outer rotation that had no important progress. About 80 % of shoulders (24 of 30) there was a satisfactory observation. As a result reverse shoulder arthroplasty for revision operation is a proper method when instability, mixture of bone loss and cuff deficiencies existed as compared to unconstrained prosthesis [30].

2.3 Developments of Shoulder Joint Implants

Shoulder arthroplasty was introduced in 1893 by Jules Emile pe'an who is a French surgeon. A platinum and rubber implant was used for a 37 years old patient by the surgeon and the amount of strength and motion range had a good result just after the operation. After the 24 mounts, infections were diagnosed and implant had been removed. After 11 out of 12 patient with fracture problem treated in 1955 with proximal humerus arthroplasty medication shoulder arthroplasty became common. All shoulder arthroplasty was first done in 1977 by Marmor [30]. In 5 of Marmor's patient with rotator cuff tears, a transcendent migration was seen which led him to the proposal of total shoulder replacement. There are three different design types of total shoulder implants by Neer [30]. With one of the designs there was rotator cuff reattachment problem because of oversized ball. On the other hand in the second kind (Mark 2) the size of ball changed to the smaller one for solving rotator cuff problem. Neer tried to get rotational and movement in third type that is called (Mark 3) by adding axial rotation to the stem. At the end, Neer stopped designing prosthesis in 1974 this result just constraint alone is not sufficient to recoup for a nonfunctional rotator cuff. The same researchers designed other method of implants with fundamental root and some

rules but all of them didn't appear to work because of some failures like scapular fracture.

So that they decided to present another type with reverse ball-and-socket design. They tried to enhance the development of implants using necessary modification for fixation configuration between 1972 and 1978. Kessel in 1973 [30] used a screw in the middle of glenoid and lateralized middle of rotation. In 1975, Fenline [30] thought that enlarged ball-and-socket would increase deltoid lever arm for absent rotator cuff. Paul Grammont invented a new system which he could put majority of his efforts on four keys features [30]. Inherently stability for the prosthesis, concave shape for supported part and convex shape for weightbearing. Grammont had three types of patterns of reverse prosthesis [31]. First reverse shoulder implant model, he designed it in 1985, included just 2 parts, they were made of metal or ceramic, which was fixed using ceramic and polyethylene socket. Because of unsatisfactory consequence he changed some modifications for the next model for instance changing glenoid to an uncemented system because of several failures, using a central peg and some screws of divergent directions for glenoid fixation.

The second model that called Delta 111 was presented in 1994 [31] [32]. Grammont led to general his final model in 1994 that contained direct modifications in humeral part. The basic design of reverse shoulder arthroplasty was unsuccessful so the concept of this method introduced from 1970s.

2.3.1 Reverse Shoulder Implant Components

In general, reverse shoulder prosthesis includes four or five main parts. One of the parts is glenoid baseplate which is disk shaped coated by hydroxyapatite starting fixations are done with primary peg and four or six holes this can be different in

different companies. The target of the divergent screw is to react the shearing forces while abducting. Glenosphere as another component is like a sphere that is made of cobalt-chrome normally. The glenosphere will be placed in baseplate and also it doesn't require screw for fixation. There are no screws for fixation and it press fitted on to humeral neck, and it can be mentioned as fourth main part. This part is made of titanium alloy with a hydroxyapatite-coated surface and polished. Different size are used depend on size of humeral cup. At the end the last part is humeral stem. It is generally made of titanium alloy or cobalt-chrome for cemented or uncemented fixation. For cemented fixation every parts of the process is the same but just before adding stem. Humeral canal is filled with doughy cement [33][34]. It is necessary to check the component's quality for making sure about reliability of product, and also is important for medical materials lie prostheses to ensure that there is no failure or malfunctioning when they're implanted. Simulating each movement of natural joints is necessary, they are supposed to work for lifelong and it is difficult to test prototype for such a period of time. There are 2 types of statics which are experimented in subluxation mode and they are mode and three dynamics. Shoulder glenoid shear (ASTMF 1829) is an Endolab shoulder prostheses testing to calculate the static shear disassembly force of modular glenoid components [34].

2.3.2 Mechanical Test of Implants

In order to make sure about the reliability and longevity of products, it is essential to control the component's quality and also it is more important for medical component like prostheses to ensure that there is no failure or malfunctioning when they are implanted in patient's body. There are some common testing standards such as International, American, British and European standards. In addition to those standards, simulating movement and motion of natural joints are essential.

Additionally, prostheses are supposed to work for lifelong and it is difficult to test prototype for such a long period of time for shoulder prostheses. ASTM F2028 is one of the operated tests, that EndoLab® performs for dynamic evaluation of glenoid loosening. There are two statics that are tested in subluxation mode and three dynamics, which are tested up to 100,000 cycles in loosening mode. Pivoting or rocking of glenoid component due to cyclic displacement of humeral head to opposing of glenoid rim is measured in this experiment [35]. Shoulder glenoid shear (ASTM F1829) is another EndoLab® shoulder prostheses testing to determine the static shear disassembly force of modular glenoid components. To compare with the other prostheses and as a design validation it is also used [36]. There are also another exclusive testing for shoulder prostheses such as wear test, range of motion, porous coating, fatigue test and modular connections but they are restricted to company, so reaching to the information is difficult.

2.3.3 Common Complications Following Shoulder Joint Arthroplasty

Impingement of the medial border of humeral cup against the scapular neck during adduction and existence of polyethylene wear debris, which cause osteolytic reaction are main complications after the shoulder arthroplasty. First siveaux described in 1997 [37]. Researchers are not sure about evolution of scapular notching where radiographic results are arguable. Result of some researches has clarified the necessity of inferior replacement of glenoid part to prevent the impingement and scapular notching. High grade notching was between 15% to 20% of shoulders applying this change [38][39][40]. Instability of reverse shoulder arthroplasty has some main reasons for example insufficient tension in deltoid muscle that causes global decoaptation, which is an abnormal gap between ball-and-socket.

After reviewing the literature and improving our knowledge about the complications of shoulder joint prosthesis after the arthroplasty, we have decided to work on the impingement and micromotion problems of the shoulder joint prosthesis components during articulation. This study is aimed to be performed to provide insight into the reason of impingement based on component design and improve the further designs. Therefore, FEA is used in this thesis which is one of the most commonly used program to perform sophisticated numerical analysis of the prosthesis and distribution of stresses.

Chapter 3

METHODOLOGY AND MATERIAL PROPERTIES

3.1 Developing 3D Models Using SolidWorks

For the purpose of this study, SolidWorks software has been used to model and manipulate the components of the reverse shoulder implants. Similar profiles that are being currently used in implants have been designed and the geometrical properties of each part have been carefully implemented. Shoulder joint structure for analysis is consisted of bony scapula and humerus and baseplate, screws, glenosphere, humeral cup and humeral stem as implant components. The implementation and design of each part is explained in details in the following subsections.

3.1.1 Scapula Bone

The scapula part has been imported into the SolidWorks software and its geometry has been manipulated for further assembly. Then the bone parts imported into the Geomagic software and surfaces modified to obtain a smooth surface and modify the number of trangles (Figure 1).

Figure 1: Scapula Bone

3.1.2 Humerus Bone

Humerus has also been imported into the SolidWorks software to obtain and visualize the 3D model. The same procedure applied to the humeral bone and triangle numbers as well as the surface have been modified in the Gomagic software. (Figure 2).

Figure 2: Humerus Bone

3.1.3 Baseplate Component

To generate the 3D model of the baseplate, implant parts should be imported into softwares separately. First a cylinder that is 30 mm in diameter and is 30 mm long has been modeled as 3D. Two 5 mm wide holes are carved out on its surface on opposite

sides by using Hole wizard features. Secondly, cylinder with 18 mm diameter and 4 mm long is designed containing a hole in its center with diameter of 7.5 mm and 7 mm length. For the screw part with 30 mm length a third cylinder is considered and by using the draft feature it is converted to a cone shaped. Afterwards the screw is generated with helix feature. Finally by proper using of the fillet feature and assembling the three 3D outputs the baseplate model has been obtained (Figure 3). At the end of the study, in appendix 2 [15] [16] the details of this modeling is viewable.

Figure 3: Baseplate Component

3.1.4 Glenosphere Component

A semicircle with 36 mm diameter has been created and with revolved boss/bass feature, it is rotated and converted into a hemisphere. For the second end a cylinder with 9.5 mm length and 7.5 mm diameter has been formed. By adding these two parts to the end of each other the glenosphere has been generated as one of the most important component of the reverse shoulder joint prosthesis (Figure 4). Also the detailed representation of the glenosphere design could be observed in appendix 1 [15] [16].

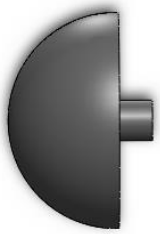

Figure 4: Glenosphere Component

3.1.5 Humeral Cup

To form the humeral cup, similar to previous sections two cylinders and one hemisphere have been created. The bigger cylinder has 42 mm diameter and its top has 8 mm and its bottom has 3 mm length as it could be seen in Figure 5. Also a 36 mm diameter shell has been defined on the cylinder by using shell features. Second smaller cylinder has 34 mm diameter and 2 mm height. Hemisphere is the last part for this assembly which is a 35 mm diameter hemisphere. The final assembled model is shown in Figure 5. The details of the modeled humeral cup are available in appendix 3 [15] [16].

Figure 5: Humeral cup

3.1.6 Humeral Stem

Firstly, a 42 mm diameter hemisphere has been produced and it is similarly converted to spherical shell with 35 mm inner diameter which was performed earlier. The second

part has been sketched separately in another 2D sketch by drawing two parallel lines with 6 mm distance of each other and two different lengths of 30 mm and 35 mm and they are connected together by two arcs. It is transformed to the 3D part by extruded boss/base feature. Again the final Humeral Stem is created by parts assembled to one part (Figure 6). appendix 4 [15] [16] contains the details of this component`s modeling properties.

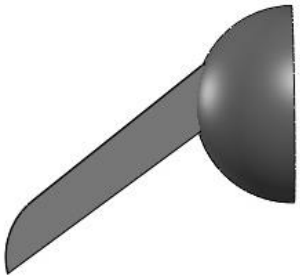

Figure 6: Humeral stem

3.1.7 Screw for Implant Fixation

The screw was developed by firstly a hemisphere with 6 mm diameter is created and followed by using the line feature and extruded cut feature one side of hemisphere has been cut. In the plane of the output shape from the hemisphere, a 3 mm diameter circle is created and with the extruded boss/bass feature it is changed to the cylinder and 26 mm length is considered for cylinder. The end of the cylinder with fillet/chamfer feature changed to the cone shape. Finally, by using helix and spiral feature in curves option, threads of screw have been created (Figure 7). Details of the design of this component is also available in appendix 5 [15] [16] section at the end of the study.

Figure 7: Screw

3.1.8 Final Assembly of the Reverse Shoulder Prosthesis

To finalize the 3D model of the reverse shoulder joint, all different parts described beforehand are either scaled down or up in order to fit in the assembly and are relatively in scale with each other. Figure 3.8 illustrates the final assembly of the 3D model created for the analysis.

Figure 8: Final Assembly of the Reverse Shoulder Prosthesis

3.2 Developing Finite element Model of the Reverse Shoulder Prosthesis

Scientifically, engineers and clinicians should have a common language to understand the complications of prosthesis. The Finite Element Analysis is one of the used software which provide wide range of information meaningful for both engineers and clinicians. Finite element is a very common and useful method in engineering which

is being used frequently in many different scientific projects, mostly engineering, from the design and analysis of areophane engine to stability analysis in civil engineering for buildings and bridges. Hence most of the analytic software available now for design purposes are based on finite element method appropriate modifications. Finite element could be used to analyze the stability of any 2D and 3D model in different load systems. Hence this study also uses ANSYS, FE analysis method to apply the analysis.

In order to increase the efficiency and decrease the computational complexity, since it does not affect the result accuracy more than allowable limits, some details were neglected or simplified. Anyhow adding more detail would increase the accuracy and it could be carried out in future studies, but as far as this research concerns the stress distribution on critical areas, it was found appropriate to simplify the models and obtain the results efficiently.

3.2.1 Meshing Tool

Several studies have been carried out to compare alterations between different types of meshing in order to illustrate their advantages and drawbacks. In order to choose the appropriate type of meshing, two important issues have to be considered. First one is the representation the level of domain. This aspect is actually alteration between final designed meshed domain and the areas or volumes of the real design subject. Second issue that should be considered for choosing the proper meshing method is Quality that regards to the association between the angles, length of edge, distance between specific element's point and etc. Because of the important role of element quality issue on the simulation reliability, it has been chosen for the key indicator of the meshing method.

Hence, two factors for quality of meshing is considered, first the Ratio between the maximal and the minimal distance for each element is known as aspect ratio (AR) which is the distance between faces of the elements. Optimum element should gain a unit value as its aspect ratio (AR=1), and if it gains higher values the element can be deformed. The second parameter, which is wrapping factor (WF), the distances of the face's nodes to an average plane needed to be computed. Ideal element is WF which is equal to 0 and it is achieved when all the nodes are coplanar. By increasing the WF value, there will be worse quality of the face and element.

Triangles and rectangles for two- dimensional problems, tetrahedral and hexahedral for 3D problems are commonly used. Tetrahedral meshes, which are most used for medical field, are considered for the assembly model in this study.

3.2.2 Material Specifications

Mechanical material specifications are demarcated for each different part regarding to appropriate materials that are used by beforehand studies. Hence all constituents are presumed to be elastically linear and isotropic materials, two of elasticity parameters can provide the other parameters. The formula for each elasticity parameter is as following [28] [29].

In following equations K is the bulk modulus which is could be described as the ratio of the infinitesimal pressure growth to the resulting comparative reduction of the volume. E is the Young`s modulus which is also known as tensile modulus and it is defined as a mechanical property of linear elastic solid materials. G represents the shear modulus or modulus of rigidity and it is the ratio of the shear stress to the shear strain. Finally υ represents the Poisson's ratio and it is the negative ratio of transverse to axial strain.

As it is observable in bellow equations these four parameters could be obtained from each other, using different equation structures (as cited in [44]).

Bulk modulus (K):

$$K = \frac{2G(1+\nu)}{3(1-2\nu)} \tag{3.1}$$

$$K = \frac{EG}{3(3G-E)} \tag{3.2}$$

$$K = \frac{E}{3(1-2\nu)} \tag{3.3}$$

Young's modulus (E):

$$E = \frac{9KG}{3K+G} \tag{3.4}$$

$$E = 3K(1-2\nu) \tag{3.5}$$

$$E = 2G(1+\nu) \tag{3.6}$$

Shear modulus (G):

$$G = \frac{3K(1-2\nu)}{2(1+\nu)} \tag{3.7}$$

$$G = \frac{3KE}{9K-E} \tag{3.8}$$

$$G = \frac{E}{2(1+\nu)} \tag{3.9}$$

Poisson's Ratio (υ):

$$\nu = \frac{3K-2G}{2(3K+G)} \tag{3.10}$$

$$\nu = \frac{3K-E}{6K} \tag{3.11}$$

$$\nu = \frac{E}{2G} - 1 \tag{3.12}$$

3.2.2.1 The Scapula Properties

As the scapula is a bone part used in this project, the bone properties have been found from the literature and are defined in Table 2.

3.2.2.2 Glenosphere Component

Generally, CoCrMo (Cobalt-chrome or cobalt-chromium) alloy is considered for glenosphere component. Mechanical properties of CoCrMo are defined in Table 1. This material is commonly used in artificial implanting due to its high wear-resistance and biocompatibility (non-toxic and is not rejected by the body).

3.2.2.3 Baseplate Component

Baseplate`s material is chosen to be Titanium alloy (for medical uses titanium is alloyed with about 4%-6% aluminum and 4% vanadium), also because of its biocompatibility as its properties are given in Table 1.

3.2.2.4 Humeral Stem Component

The same titanium alloy considered for the humeral stem. Stiffness behavior of this part is defined as rigid. So, there is no meshing and analysis on this part. Titanium alloy properties are given in Table 1.

3.2.2.5 Humeral Cup

Ultra-high molecular weight polyethylene (UHMWPE) is one of the most commonly used materials in biomaterials for over 40 years and it is chosen for the humeral cup. Starting from 2007 UHMWPE manufacturers integrated this material with antioxidants to be used in knee and hip implants and arthroplasty. Polyethylene specification is described in Table 1.

3.2.2.6 Humerus Bone

Similar to the scapula bone, for humerus bone, the specifications from the literature are chosen (Table 1). As the aim of this project is stress and strain behavior analysis at

glenoid part and glenohumeral joint, stiffness behavior of humerus part is considered as rigid and there is no meshing and analysis of this part. Basically, the bone parts are not involved in the finite element analysis in this study.

3.2.2.7 Screws

Two screws are used for fixing the baseplate into the scapula bone. Again Titanium alloy is considered as the material of screws because of its biocompatibility and acceptable material spesifications. Properties of the titanium alloy are given in Table 3.1.

Table 1: Material Properties (Mechanical Properties of Engineered Materials; Wole Soboyejo; 2002) [44]

Property	**Unit**	**Titanium alloy (4%-6% aluminum and 4% vanadium)**	**CoCrMo alloy**	**UHMWPE**	**Bone**
Density	Kg m^{-3}	4430	7900	950	2100
Elastic modulus (E)	Pa	1.138E+11	2.3E+11	1.1E+09	1.42E+10
Poisson ratio (υ)	_	0.342	0.29	0.42	0.3
Bulk modulus (K)	Pa	1.2004E+11	1.9167E+11	2.2917E+09	1.1833E+10
Shear modulus (G)	Pa	4.2399E+10	8.8462E+10	3.8732E+08	5.4615E+09
Tensile yield strength (TYS)	Pa	8.8E+08	9.8E+08	2.5E+07	1.14E+08
Compressive yield strength (CYS)	Pa	9.7E+08	_	1.4E+07	1.20E+08

Table 2: Material of each part of the reverse shoulder prosthesis

Component	Material
Scapula	Bone
Baseplate	Titanium alloy (4%-6% aluminum and 4% vanadium)
Glenosphere	CoCrMo alloy
Humeral cup	UHMWPE
Humeral stem	Titanium alloy (4%-6% aluminum and 4% vanadium)
Humerus	Bone
Screws	Titanium alloy (4%-6% aluminum and 4% vanadium)

3.3 Kinematic Properties

To correctly model the kinematics of the shoulder implant, joints were defined to connect each component of the implant. Joints are defined one by one according to their kinematic and static necessities. On the other hand connection areas should be defined to represent the appropriate connection kinematics. The following sections are the specifications of the aforementioned connections.

3.3.1 Joints of the Prosthesis Components

On top of the scapula a fixed joint has been considered to create a rigid contact. Screws are also fixed to the baseplate. This fixed joint would not allow any relative movement between scapula and baseplate hence they will react as a single body in the system. Similarly another rigid joint is defined between the glenosphere shaft and the baseplate. A spherical joint with 3 DOF is defined in the contact point of the concave part of humeral cup and the convex part of glenosphere and the other side of the

humeral cup is fixed to the humeral stem with a fixed joint in their contact area. This system will relate the movements of humeral cup, humeral stem and humerus together. To analyze their rotatory displacements the Center of rotation for the system is assumed to be at the center of glenosphere. Humerus is just fixed to the humeral stem at one side.

3.3.2 Contacts between the Prosthesis Components

ANSYS software has numerous type of contact such as frictional, frictionless, rough and bonded and no separation. Each of these contact types has its characteristics, hence they would behave differently to different load forms.

Limitation for bonded contacts is for separation and slide in these relative movements are no allowed between surfaces are not allowed in bonded contact. Between screws and baseplate, scapula and baseplate, glenosphere and baseplate, humeral cup and humeral stem, and humerus and humeral stem bonded contact is assumed. Frictionless contact is defined between glenosphere and humeral cup.

3.4 Finite Element modeling process of Reverse Shoulder Prosthesis

This study uses ANSYS Workbench to analyze the stress and strain distribution at glenoid part and glenohumeral joint of reverse shoulder prosthesis during abduction, flexion and rotation movements. It is assumed that the ROM for the shoulder joint may be altered with reverse shoulder implant [44], also the exceeded micro-motion between scapula and baseplate, and polyethylene wear may cause failure of the implants [44][42]. Hence the aberration of the ROM of the implanted reverse shoulder prosthesis during abduction, rotation and flexion is examined to investigate the limits of contact stress and to find out the failure possibilities and their details.

The first step is to obtain the 3D components as described in earlier sections using SolidWorks software (subsections 3.1.2 to 3.1.6). Final 3D assembly model of the shoulder implant has been imported into the ANSYS for the analysis to be carried out (Figure 8). All of the characteristics explained in previous sections for the FE model, namely, material properties (Sec. 3.2.2), joints (Sec. 3.3.1) and contacts (Sec. 3.3.2) are defined for each part separately. Also materials, which are not available in default defined materials in ANSYS, are added manually to its material library.

Finite element analysis for this study is based on Tetrahedrons meshing with path independent algorithm for all parts. Two spring elements are defined to act as Anterior and middle deltoid muscles, which are attached the scapula part to the humerus parts. Spring constant of 3.3 N/mm is considered for aforementioned springs [42]. Therefore to simulate the forces at the glenohumeral joint during abduction, flexion and rotation movements these two springs will act as load source.

Chapter 4

RESULTS

4.1 Von Mises Equivalent Stress Applied for Abduction, Flexion and Rotation

Since the applied load to this complex shoulder system is in 3D, the generated stresses are similarly complex and different in each direction. Hence using the Von Mises stress combination formula the stresses in each direction can be determined. Using this results the stability of the shoulder implant can be evaluated. This is done by examining maximum Von Mises stress output on each part of the implant one by one and for different movements (Abduction, Rotation and Flexion) as described previously.

The results of the analysis are divided into three sections for three different movements as follows. In each section the aforementioned maximum combined stresses during the 4 second movements are presented and the stress distributions at most critical time of the movement are illustrated.

4.1.1 Maximum Von Mises Stress on each Implant Components during Abduction Movement

4.1.1.1 Baseplate

On the baseplate examination during abduction movement of the implanted shoulder the maximum Von Mises stress distribution in 4 seconds happens at t= 2.8 Sec. as

illustrated in Figure 9. Maximum stresses distribution on baseplate is given in Table 3 and illustrated in Figure 10.

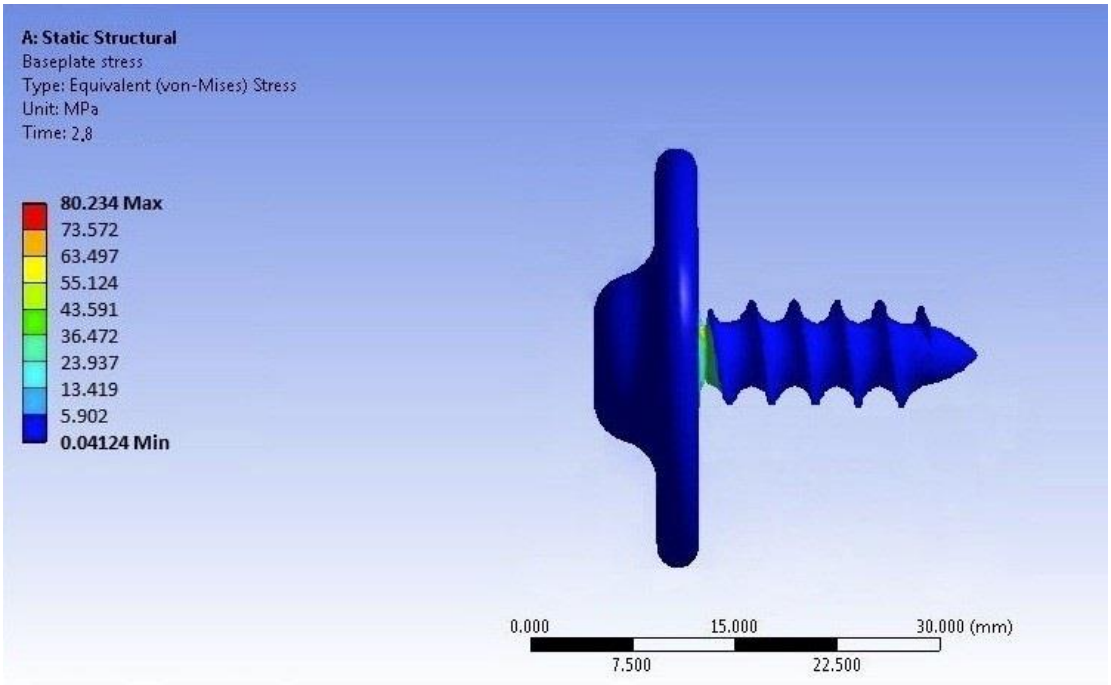

Figure 9: Maximum Stress distribution on baseplate during shoulder joint abduction at t=2.8 Sec.

Table 3: Stresses distribution on baseplate in 4 seconds during shoulder joint abduction

Time (s)	Maximum Stress (MPa)
0	0
0.4	33.23
0.8	61.72
1.2	74.36
1.6	77.133
2	79.653
2.4	82.866
2.8	84.2457
3.2	83.349
3.6	81.0915
4	77.826

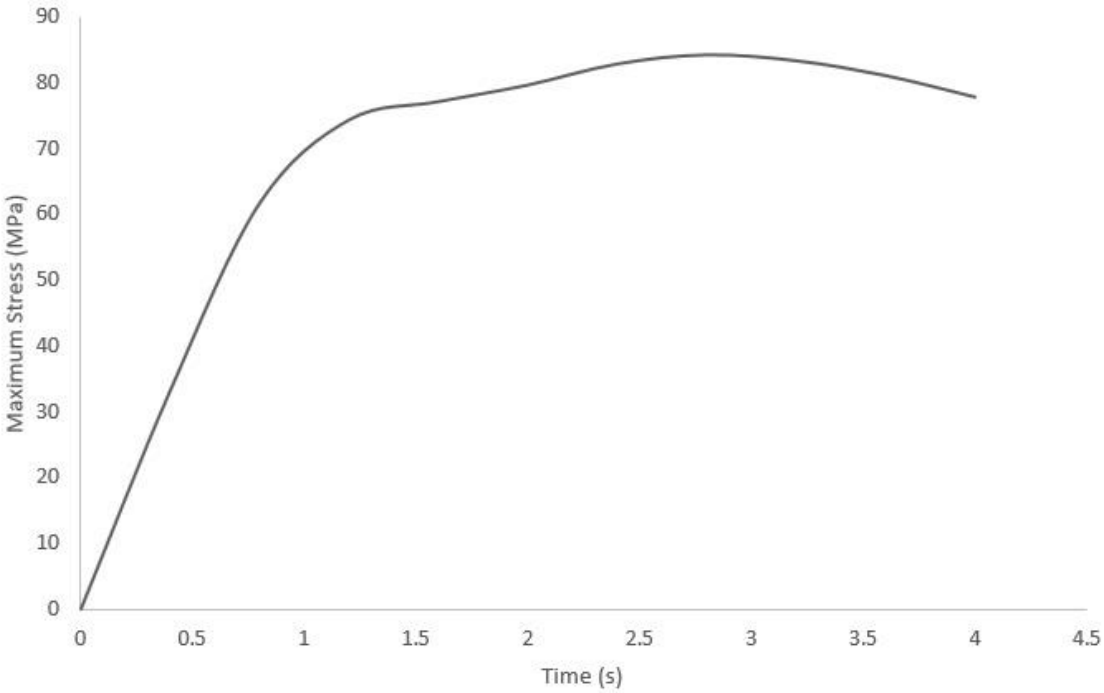

Figure 10: Stresses on baseplate in 4 seconds during shoulder joint abduction

4.1.1.2 Inferior Screw

The same result of Von Mises stress applied to the inferior screw for 4 seconds shows that the maximum stress happens at $t = 4$ Sec. as shown in Figure 11. Maximum stresses distribution on inferior screw is presented in Table 4 and it is demonstrated in Figure 12.

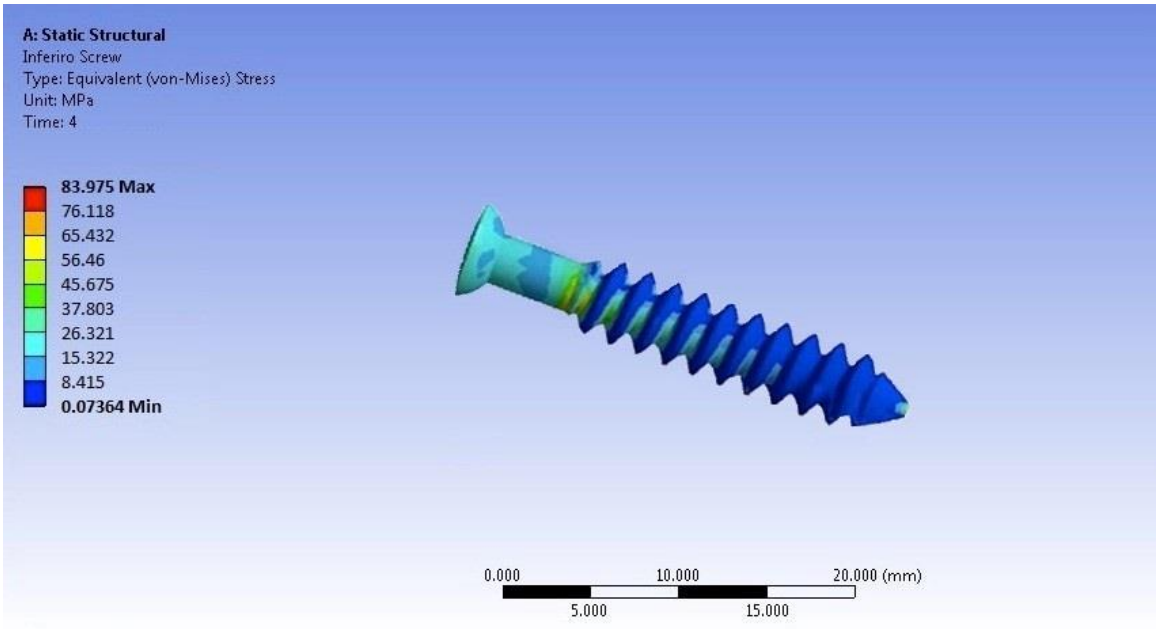

Figure 11: Maximum Stress distribution on inferior screw during shoulder joint abduction at t=4 Sec.

Table 4: Stresses distribution on inferior screw during shoulder joint abduction in 4 seconds

Time (s)	Maximum Stress (MPa)
0	0
0.4	28.6425
0.8	49.4095
1.2	61.5885
1.6	68.019
2	68.0715
2.4	69.825
2.8	73.731
3.2	77.1435
3.6	82.0995
4	88.1738

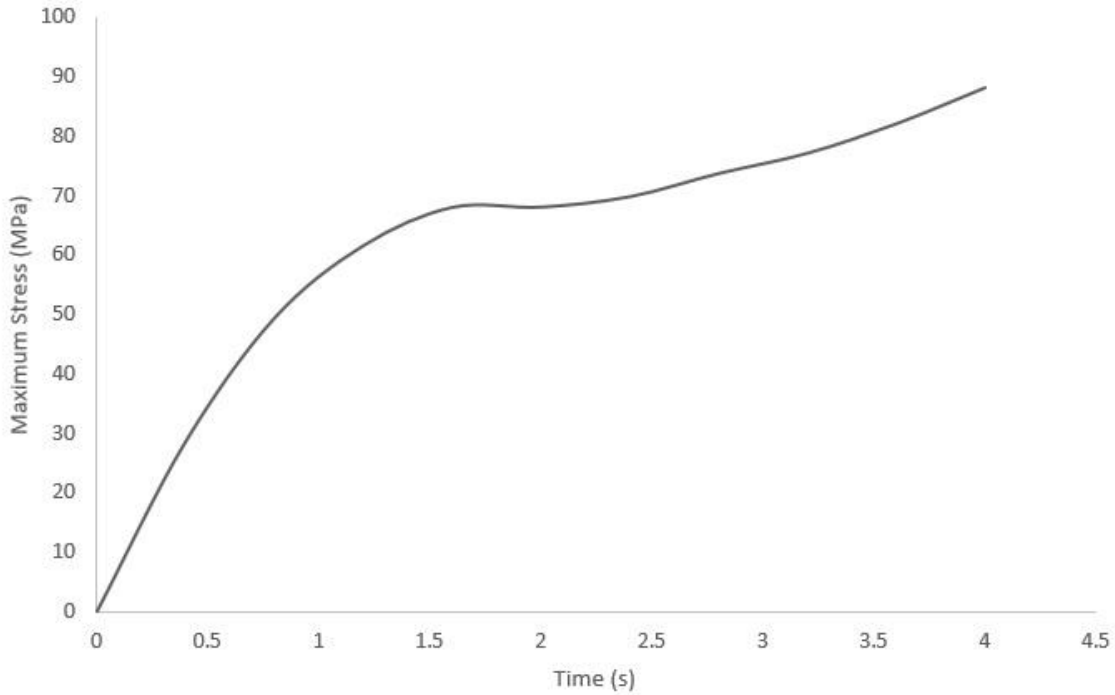

Figure 12: Stresses on inferior screw during shoulder joint abduction in 4 seconds

4.1.1.3 Superior Screw

Von Mises stress dispersal during shoulder abduction on superior screw in 4 seconds has the maximum stress at t= 4 Sec., which is shown in Figure 13. Maximum stresses distribution on superior screw is presented in Table 5 and demonstrated in Figure 14.

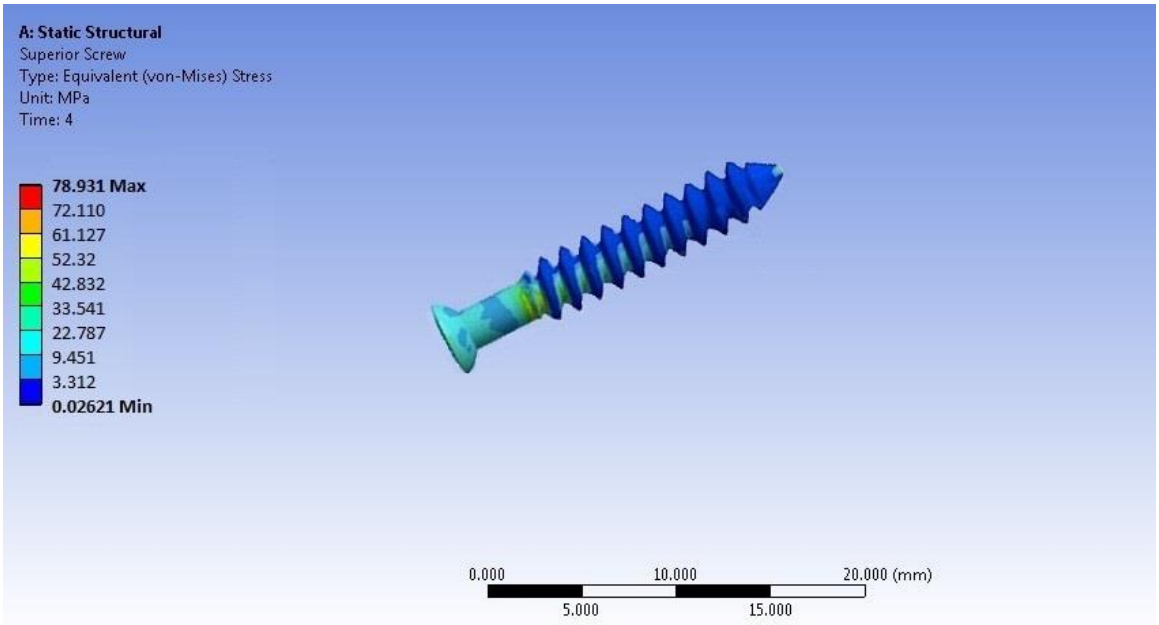

Figure 13: Maximum stress distribution on superior screw during shoulder joint abduction movement at t=4 Sec.

Table 5: Stresses distribution on superior screw during shoulder joint abduction movement in 4 seconds

Time (s)	Maximum Stress (MPa)
0	0
0.4	19.278
0.8	37.737
1.2	53.802
1.6	59.556
2	55.713
2.4	51.681
2.8	51.0825
3.2	70.9275
3.6	79.107
4	82.8776

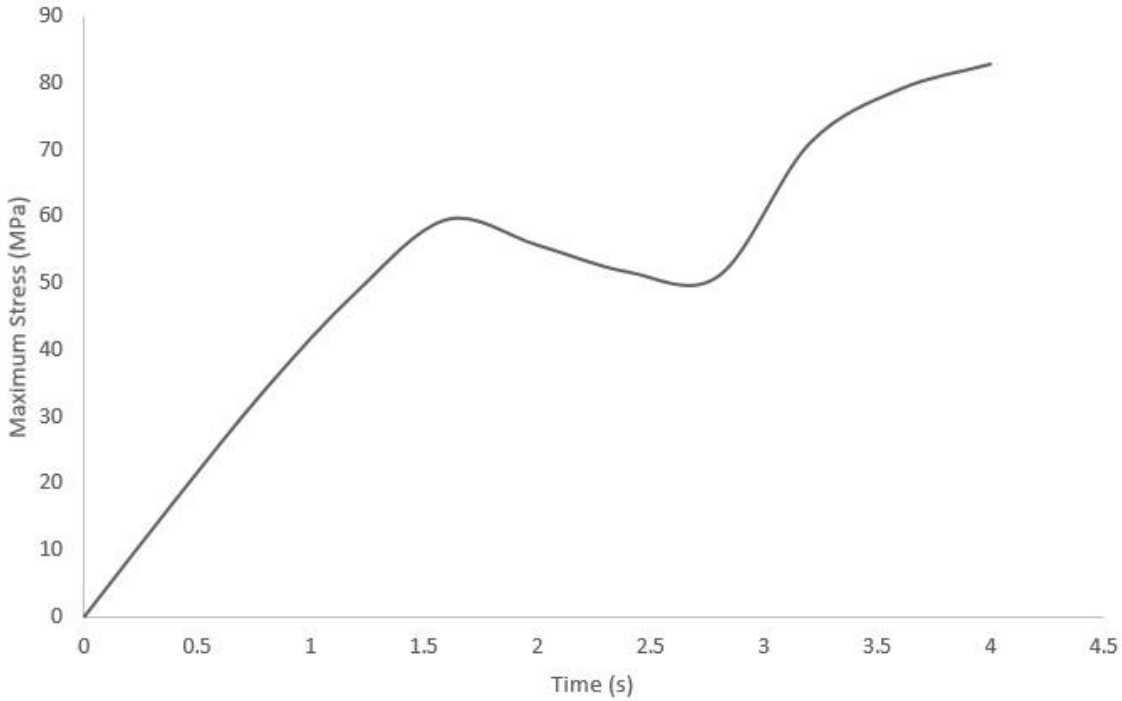

Figure 14: Stresses on superior screw during shoulder joint abduction movement in 4 seconds

4.1.1.4 Glenosphere

Following results are the Maximum Von Mises stress distribution on glenosphere during abduction movement of the shoulder implant in 4 seconds. The results shows that the maximum stress happens exactly at $t = 2.4$ Sec., which could be observed in Figure 15. Maximum stresses distribution on glenosphere is presented in Table 6 and its curved plot is illustrated in Figure 16.

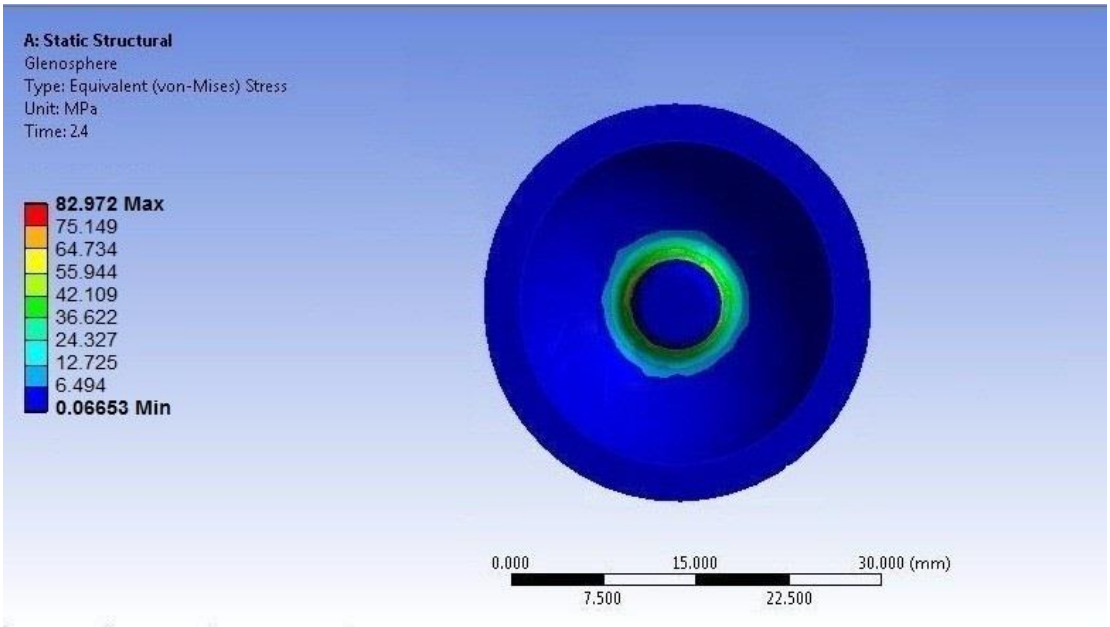

Figure 15: Maximum stress distribution on glenosphere during shoulder joint abduction movement at t=2.4 Sec.

Table 6: Stresses distribution on glenosphere during shoulder joint abduction movement in 4 seconds

Time (s)	Maximum Stress (MPa)
0	0
0.4	34.53
0.8	45.69
1.2	55.2
1.6	71.67
2	81.31

2.4	87.12
2.8	85.55
3.2	85.2
3.6	81.32
4	76

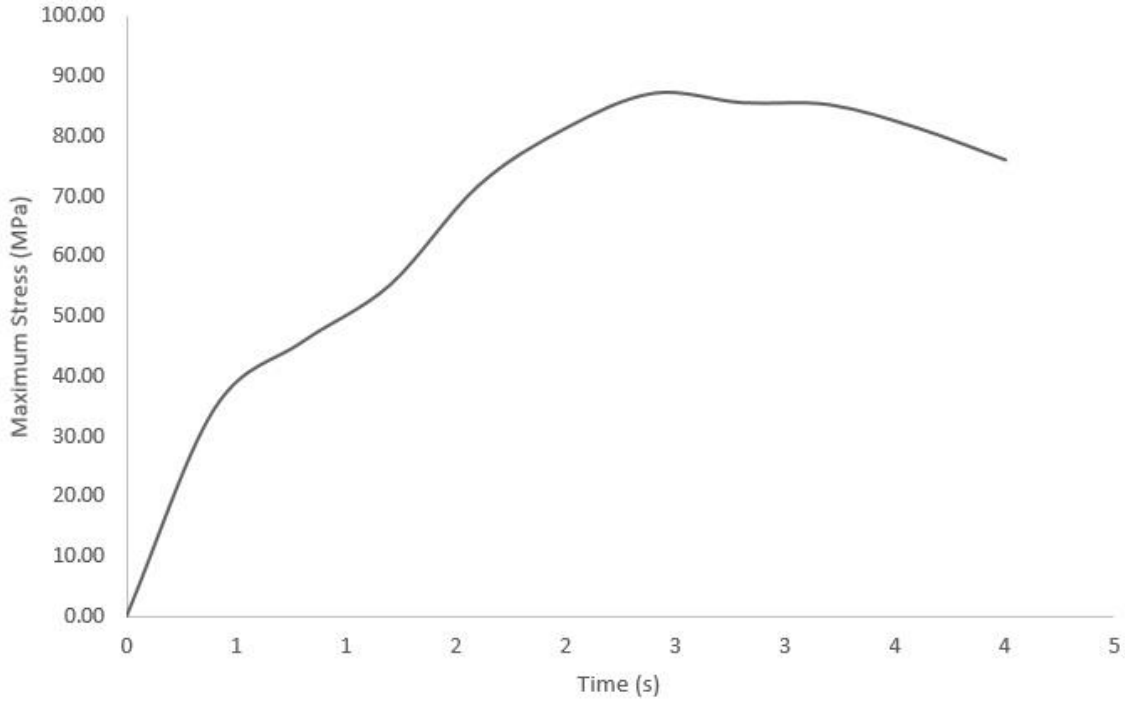

Figure 16: Stresses on glenosphere during shoulder joint abduction movement in 4 seconds

4.1.1.5 Humeral Cup

Similar results of Von Mises stress distribution on the humeral cup part of the implant during abduction movement are as follow. The maximum Von Mises stress occurred at $t = 4$ Sec., as illustrated in Figure 17. Maximum stresses distribution on glenosphere is presented in Table 7 and illustrated in Figure 18.

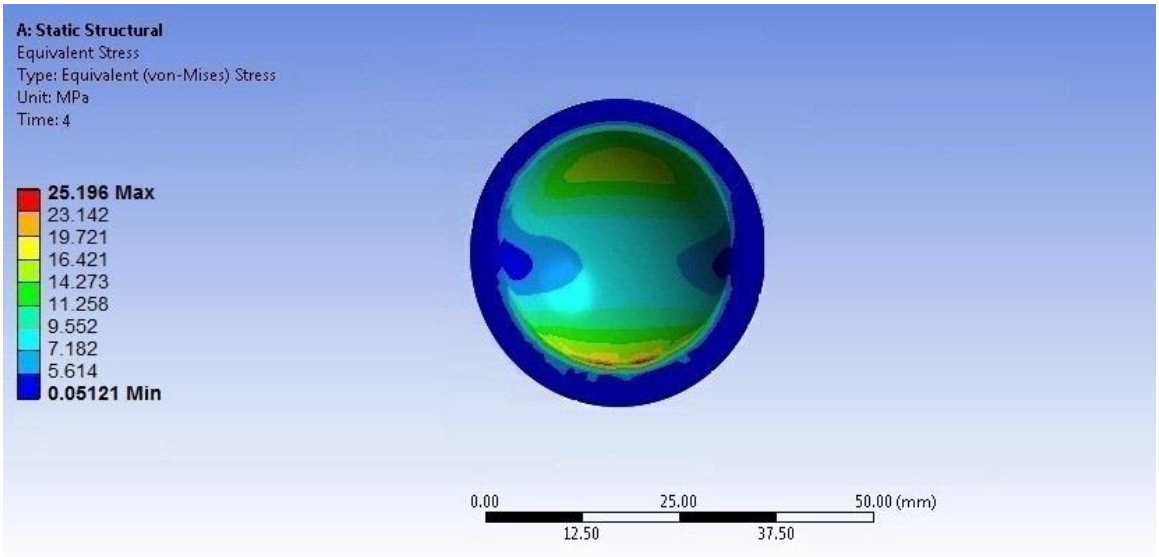

Figure 17: Maximum Stress distribution on humeral cup during shoulder joint abduction movement at t=4 Sec.

Table 7: Stresses distribution on humeral cup during shoulder joint abduction movement in 4 seconds

Time (s)	Maximum Stress (MPa)
0	0.00
0.4	5.53
0.8	8.63
1.2	11.44
1.6	14.28
2.0	15.90
2.4	17.79
2.8	19.15
3.2	20.70
3.6	23.02
4.0	26.46

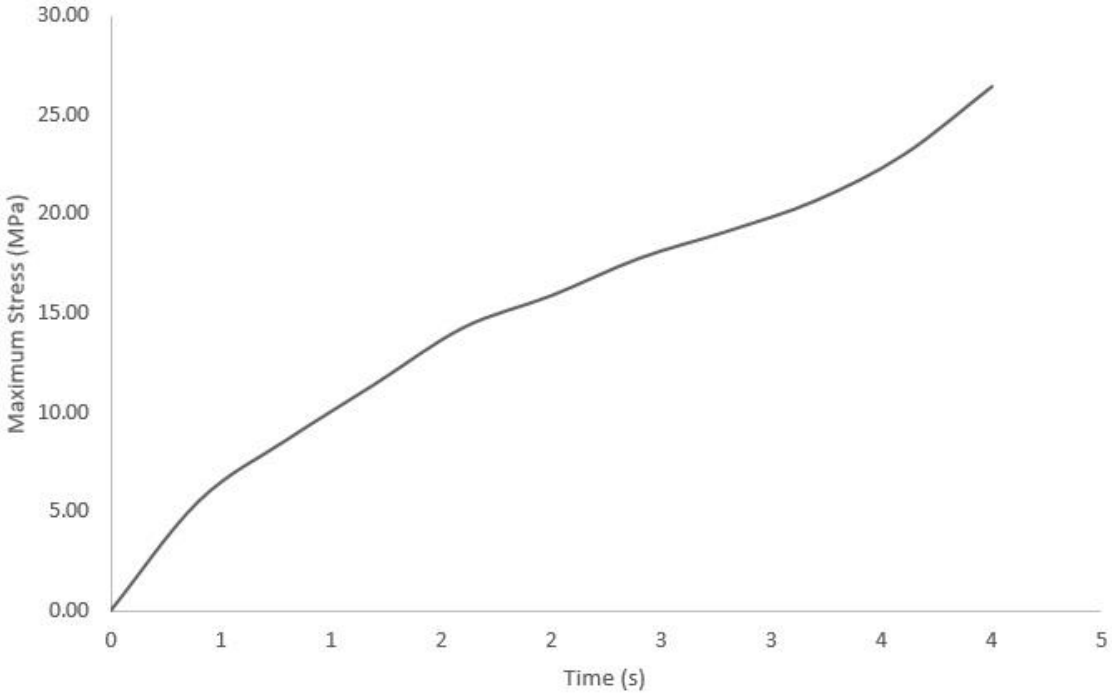

Figure 18: Stresses on humeral cup during shoulder joint abduction movement in 4 seconds

4.1.1.6 Scapula

Similarly for the Scapula the results of Maximum Von Mises stress distribution during shoulder joint abduction in a 4 second movement happens at $t = 4$ Sec., because the stress increases as time passes which is shown in Figure 19. Maximum stresses distribution on glenosphere is presented in Table 8 and illustrated in Figure 20.

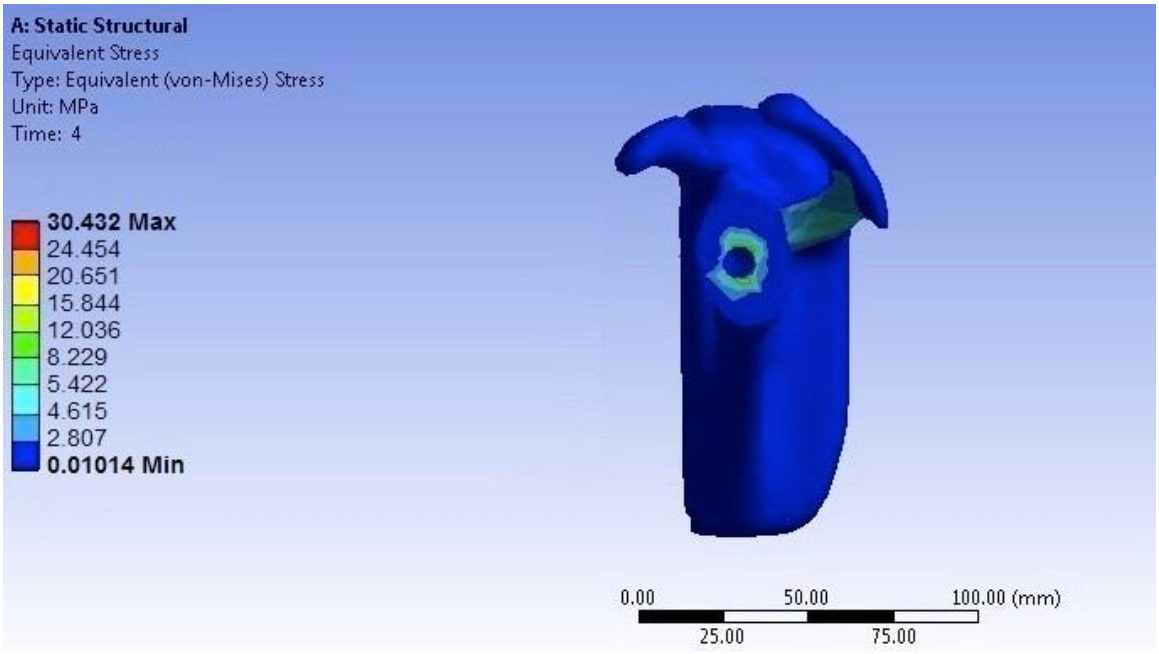

Figure 19: Maximum Stresses distribution on scapula during shoulder joint abduction at $t = 4$ Sec.

Table 8: Stresses distribution on humeral cup during shoulder joint abduction movement in 4 seconds

Time (s)	Maximum Stress (MPa)
0	0.00
0.4	3.34
0.8	4.15
1.2	6.94
1.6	10.11
2.0	11.36
2.4	12.67
2.8	17.29
3.2	21.76
3.6	30.27
4.0	31.95

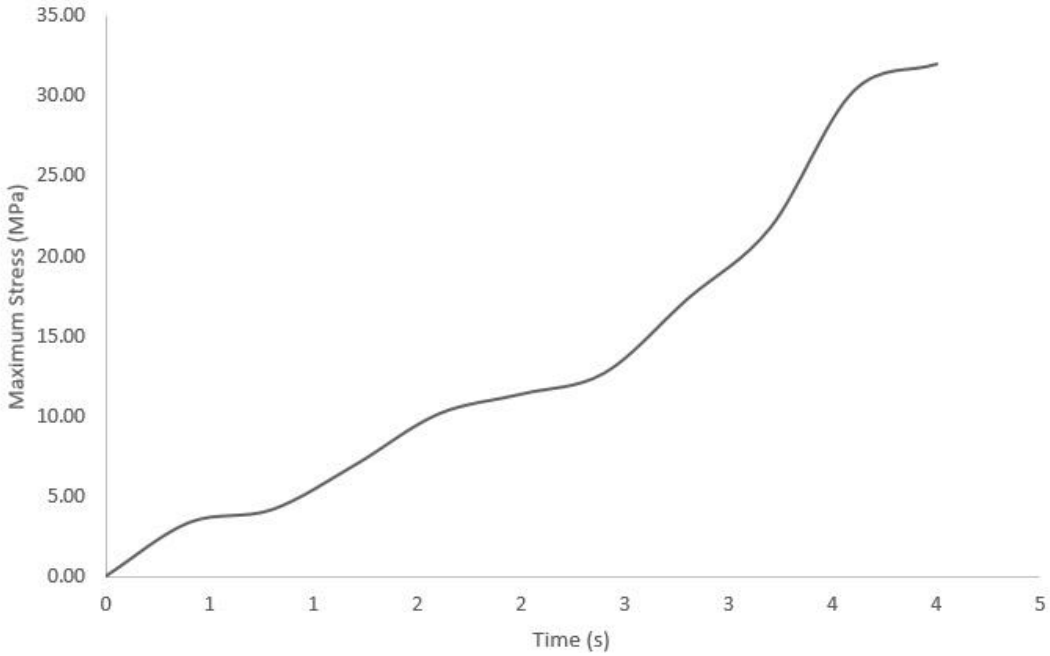

Figure 20: Stresses on scapula during shoulder joint abduction in 4 seconds

4.1.2 Maximum Von Mises Stress on each of the Implant Components during Rotation Movement

4.1.2.1 Baseplate

On the baseplate examination during rotation movement of the implanted shoulder the maximum Von Mises stress distribution in 4 seconds happens at $t = 2.18$ Sec. as illustrated in Figure 21. Maximum stresses distribution on baseplate is given in Table 9 and its plot is illustrated in Figure 22.

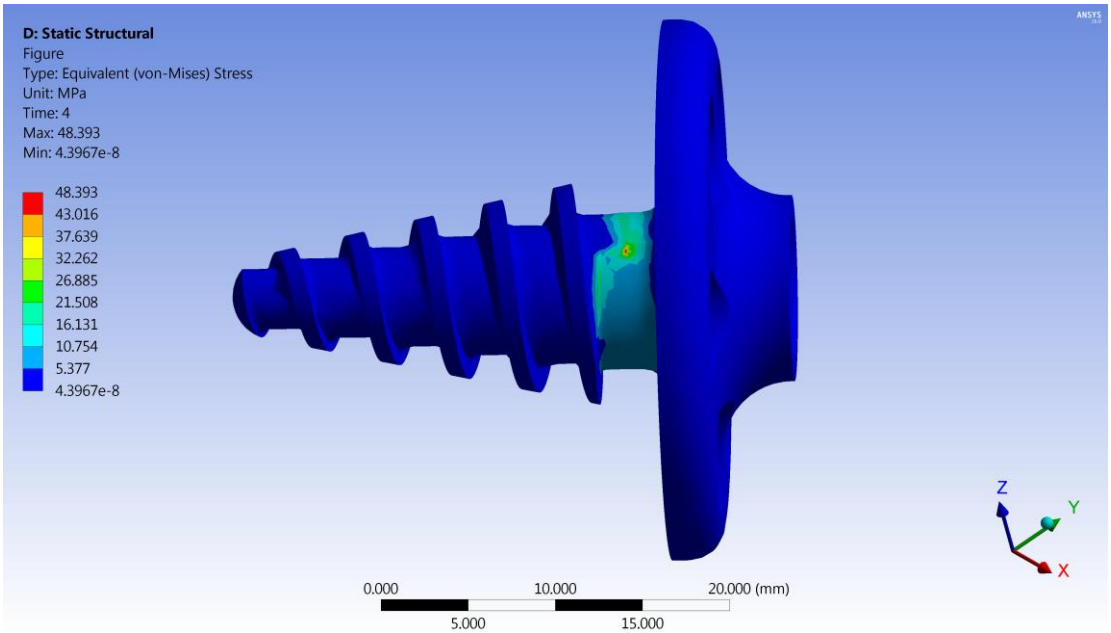

Figure 21: Stress distribution on baseplate during shoulder joint rotation at t=4 Sec.

Table 9: Stresses distribution on baseplate in 4 seconds during shoulder joint abduction

Time (s)	Maximum Stress (MPa)
0	0
0.36	43.99
0.72	52.35
1.09	60.27
1.45	69.07
1.81	77.86
2.18	77.86
2.54	69.07
2.90	61.59
3.27	57.19
3.63	52.79

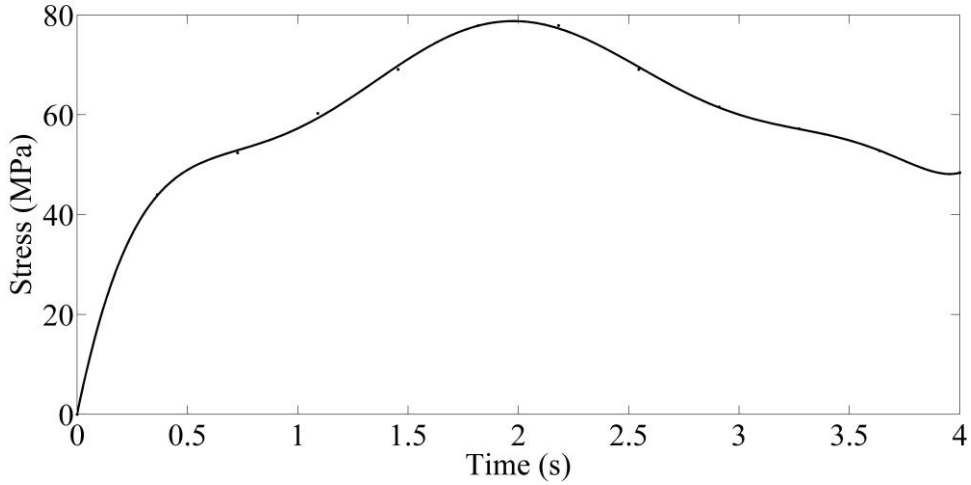

Figure 22: Stresses on baseplate in 4 seconds during shoulder joint rotation

4.1.2.2 Inferior Screw

The same result of Von Mises stress applied to the inferior screw for 4 seconds of rotation movement, shows that the maximum stress happens at t= 1.81 Sec. as shown in Figure 23. Maximum stresses distribution on inferior screw is presented in Table 10 and it is demonstrated in Figure 24.

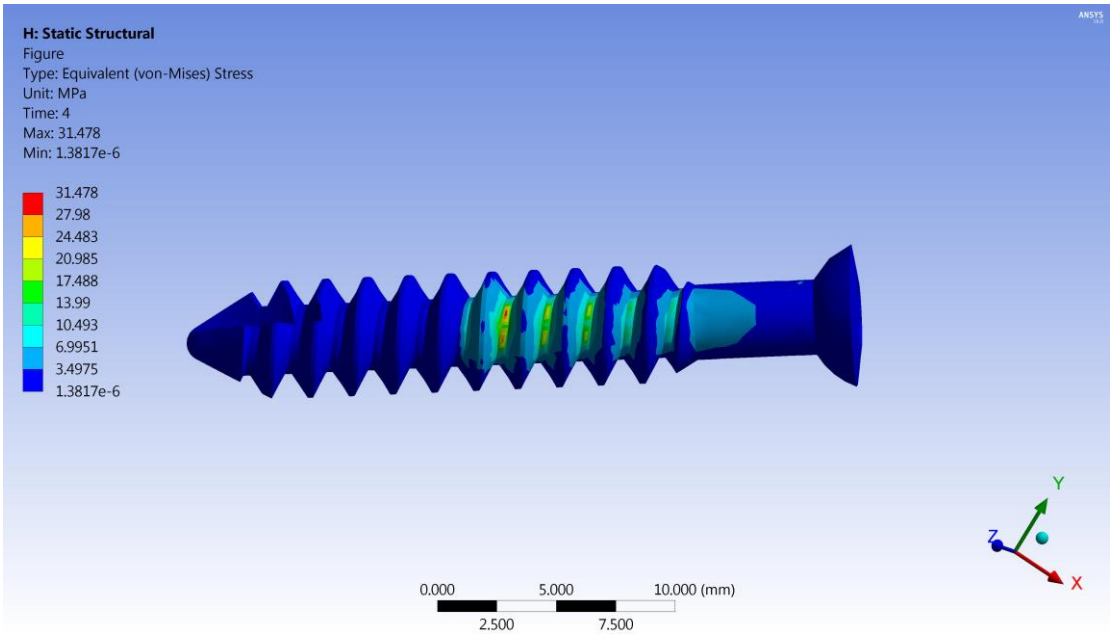

Figure 23: Stress distribution on inferior screw during shoulder joint rotation at t=4 Sec.

Table 10: Stresses distribution on inferior screw during shoulder joint rotation in 4 seconds

Time (s)	Maximum Stress (MPa)
0	0
0.36	42.92
0.72	54.37
1.09	65.81
1.45	77.26
1.81	88.71
2.18	88.71
2.54	77.26
2.90	65.81
3.27	54.37
3.63	42.92

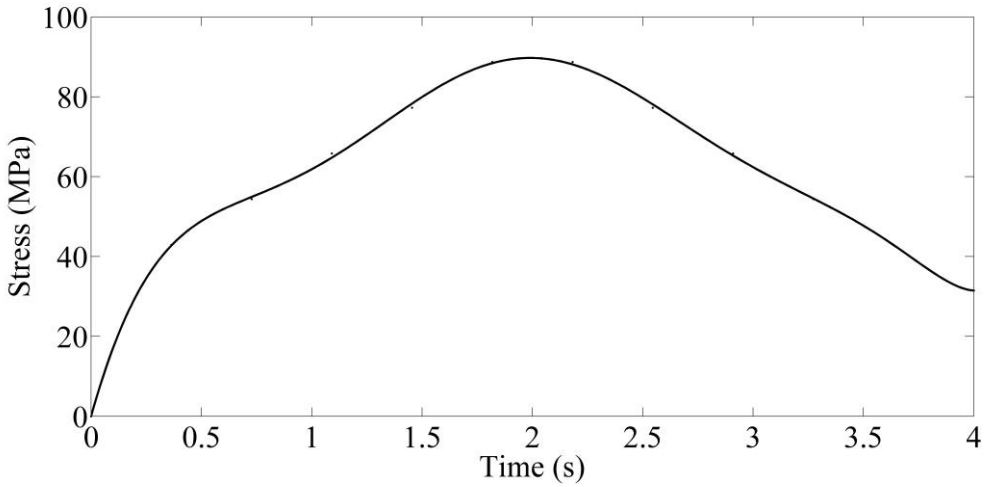

Figure 24: Stresses on inferior screw during shoulder joint rotation in 4 seconds

4.1.2.3 Superior Screw

Von Mises stress dispersal during shoulder abduction on superior screw in 4 seconds has the maximum stress at t= 4 Sec., which is shown in Figure 25. Maximum stresses distribution on superior screw is presented in Table 11 and its plot is demonstrated in Figure 26.

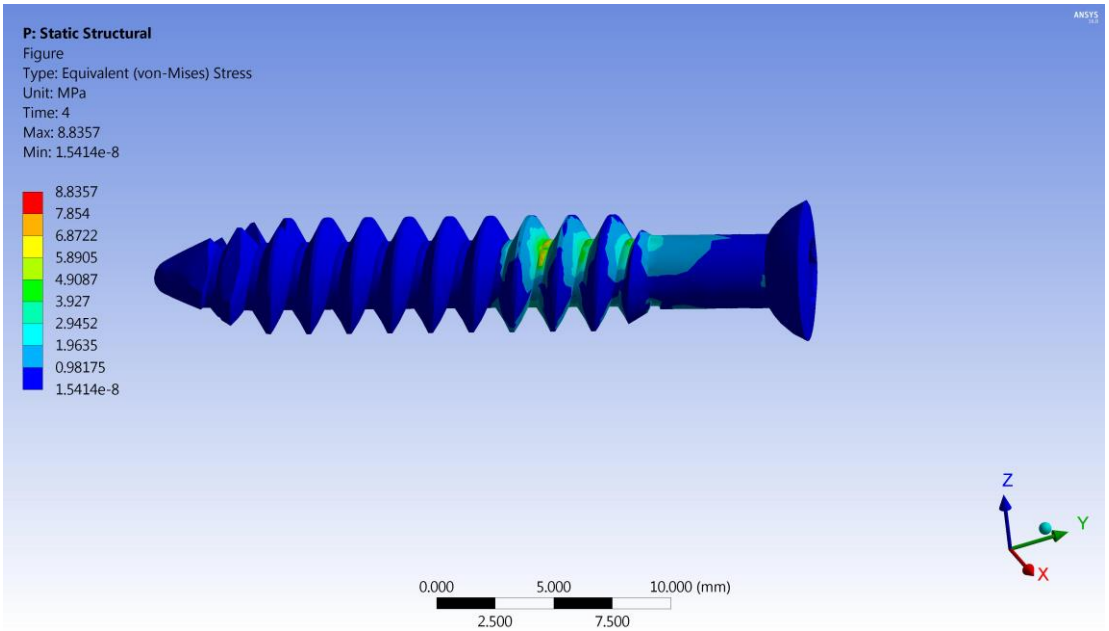

Figure 25: Stress distribution on superior screw during shoulder joint rotation movement at t=4 Sec.

Table 11: Stresses distribution on superior screw during shoulder joint rotation movement in 4 seconds

Time (s)	Maximum Stress (MPa)
0	0
0.36	38.15
0.72	54.21
1.09	69.08
1.45	80.32
1.81	91.57
2.18	87.55
2.54	68.27
2.90	48.99
3.27	34.54
3.63	21.68

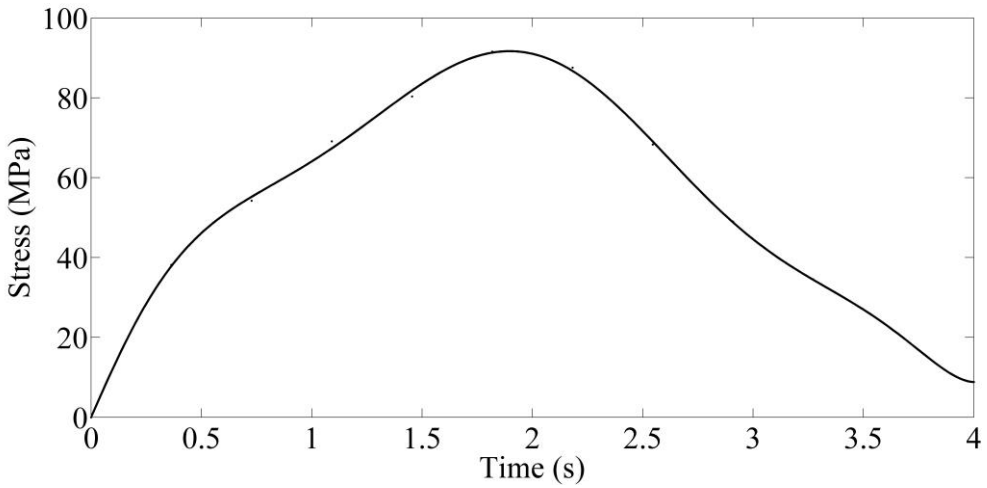

Figure 26: Stresses on superior screw during shoulder joint rotation movement in 4 seconds

4.1.2.4 Glenosphere

Following results are the Maximum Von Mises stress distribution on glenosphere during abduction movement of the shoulder implant in 4 seconds. The results shows that the maximum stress happens exactly at $t = 2.18$ Sec., which could be observed in Figure 27. Maximum stresses distribution on glenosphere is presented in Table 12 and its curved plot is illustrated in Figure 28.

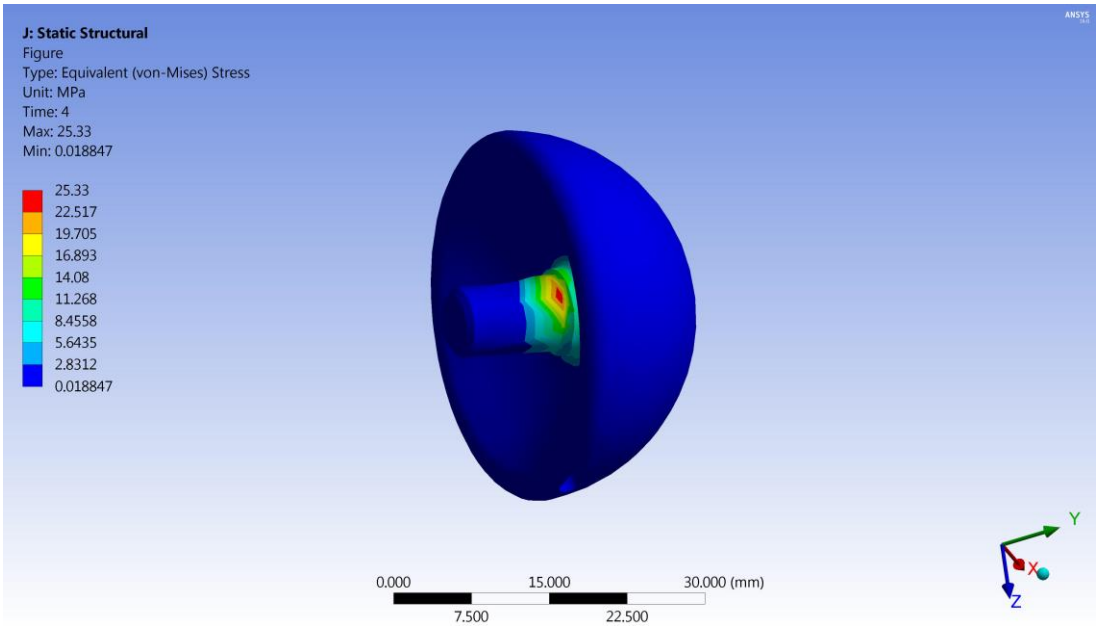

Figure 27: Stress distribution on glenosphere during shoulder joint rotation movement at t=4 Sec.

Table 12: Stresses distribution on glenosphere during shoulder joint rotation movement in 4 seconds

Time (s)	Maximum Stress (MPa)
0	0
0.36	31.08
0.73	34.73
1.09	41.89
1.45	48.3
1.81	57.56
2.18	61.4
2.54	57.56
2.9	53.72
3.27	48.35
3.63	36.84

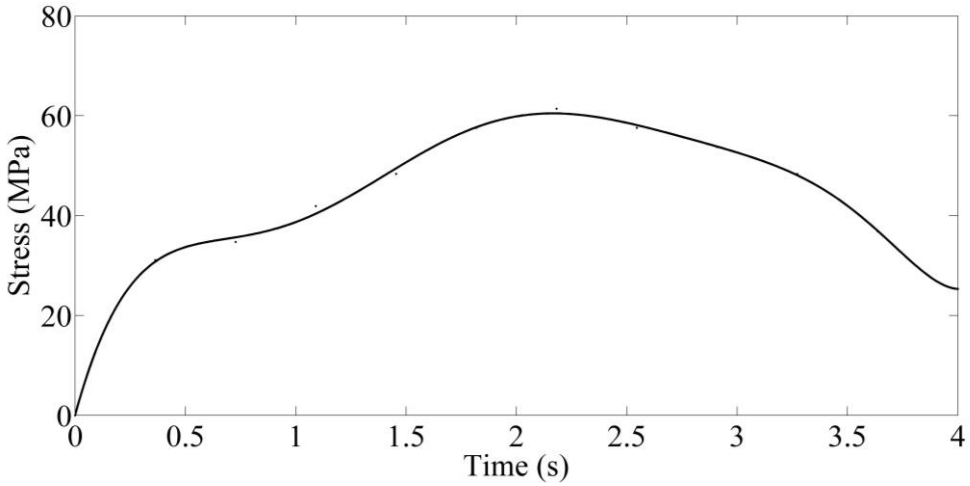

Figure 28: Stresses on glenosphere during shoulder joint rotation movement in 4 seconds

4.1.2.5 Humeral Cup

Similar results of Von Mises stress distribution on the humeral cup part of the implant during the 4 seconds rotation movement are as follow. The maximum Von Mises stress occurred at $t = 1.81$ Sec., as illustrated in Figure 29. Maximum stresses distribution on humeral cup is presented in Table 13 and illustrated in Figure 30.

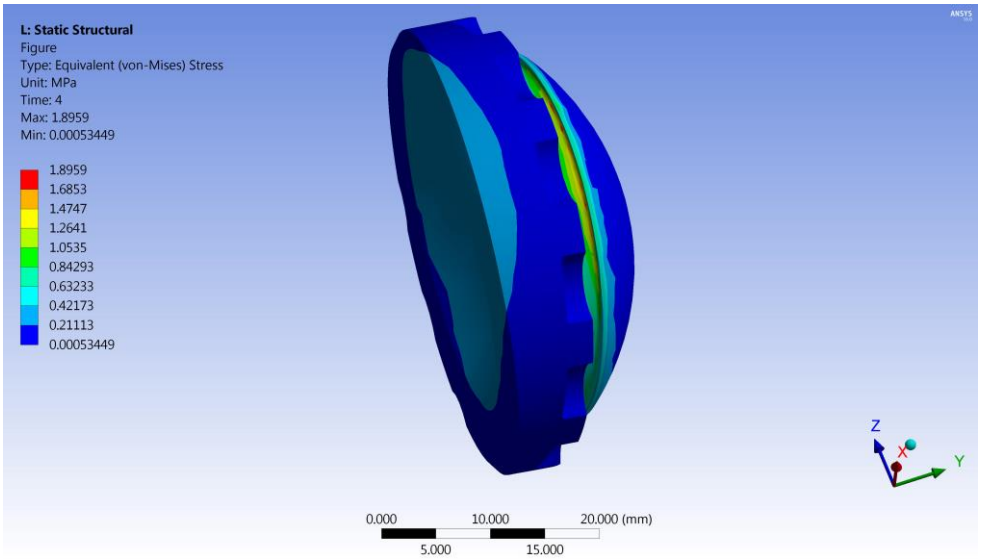

Figure 29: Stress distribution on humeral cup during shoulder joint rotation movement at t=4 Sec.

Table 13 Stresses distribution on humeral cup during shoulder joint rotation movement in 4 seconds

Time (s)	Maximum Stress (MPa)
0	0
0.36	2.15
0.72	2.95
1.09	3.42
1.45	4.30
1.81	5.06
2.18	5.06
2.54	4.31
2.90	3.42
3.27	2.95
3.63	2.32

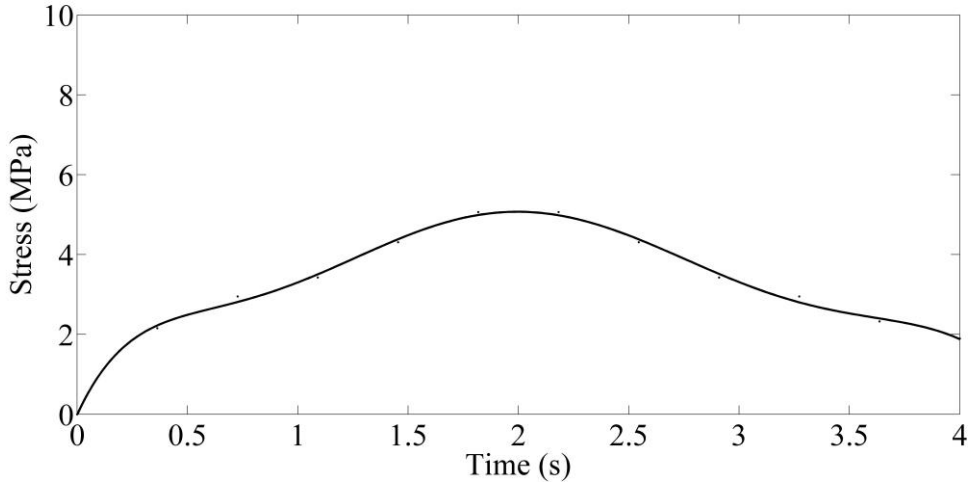

Figure 30: Stresses on humeral cup during shoulder joint rotation movement in 4 seconds

4.1.2.6 Scapula

Similarly for the Scapula the results of Maximum Von Mises stress distribution during shoulder joint rotating around its main axis in a 4 second movement happens at t = 1.81 Sec., because the stress increases as time passes which is shown in Figure 31. Maximum stresses distribution on scapula is presented in Table 14 and illustrated in Figure 32.

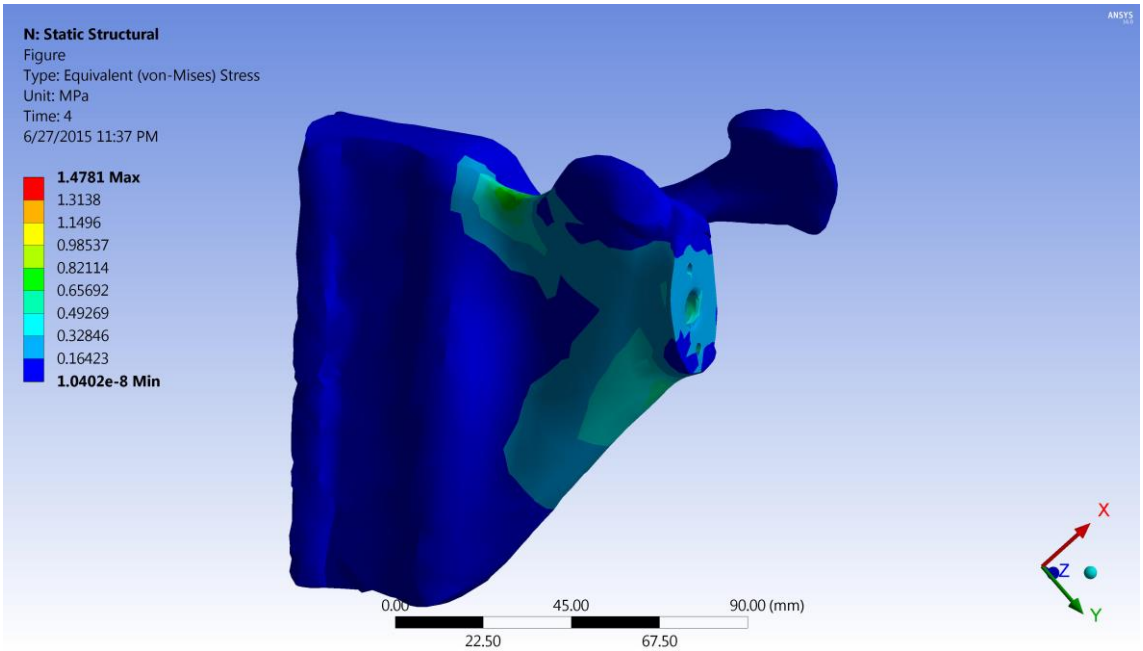

Figure 31: Stresses distribution on scapula during shoulder joint rotation at t=4 Sec.

Table 14: Stresses distribution on scapula during shoulder joint rotation in 4 seconds

Time (s)	Maximum Stress (MPa)
0	0
0.36	2.68
0.72	4.16
1.09	5.07
1.45	5.69
1.81	6.71
2.18	6.71
2.54	5.69
2.90	5.07
3.27	4.16
3.63	2.82

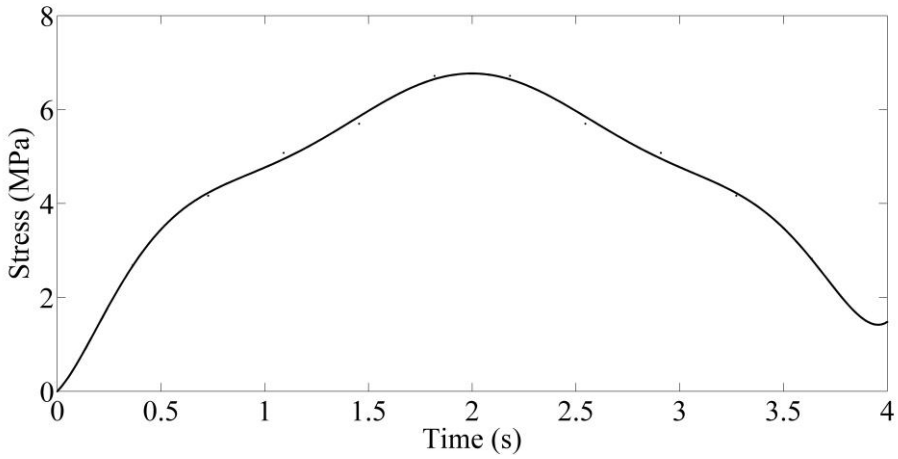

Figure 32: Stresses on scapula during shoulder joint rotation in 4 seconds

4.1.3 Maximum Von Mises Stress on each of the Implant Components during Flexion Movement

4.1.3.1 Baseplate

Examination of the flexion movement of the baseplate part of the implanted shoulder the maximum Von Mises stress distribution in 4 seconds happens at t= 4 Sec because

the stress increases as time passes as illustrated in Figure 33. Maximum stresses distribution on baseplate is given in Table 15 and its plot is illustrated in Figure 34.

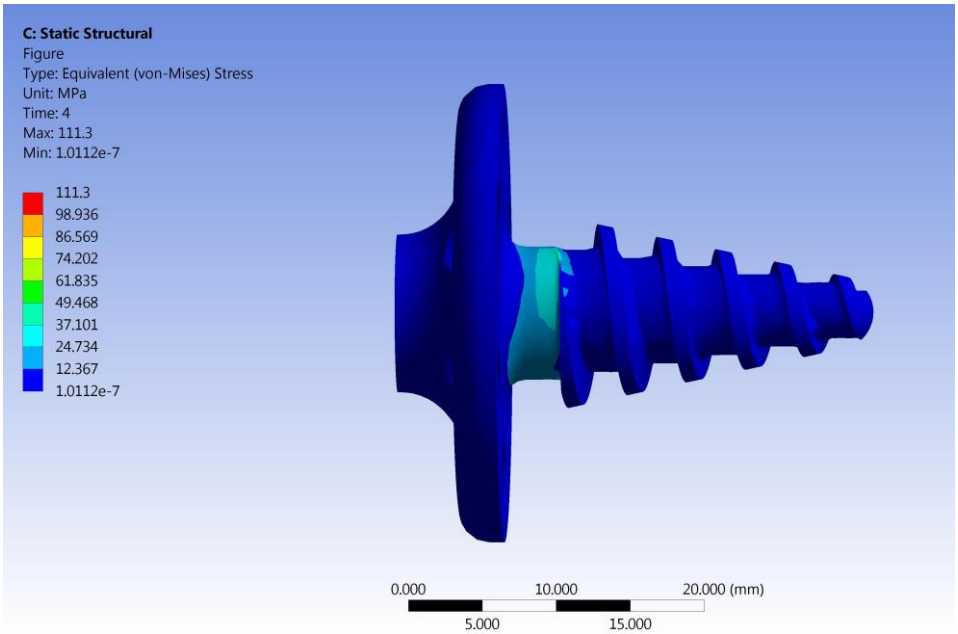

Figure 33: Maximum stress distribution on baseplate during shoulder joint flexion at t=4 Sec.

Table 15: Stresses distribution on baseplate in 4 seconds during shoulder joint flexion

Time (s)	Maximum Stress (MPa)
0.36364	43.993
0.72727	52.352
1.0909	60.271
1.4545	69.07
1.8182	77.868
2.1818	86.667
2.5455	93.706
2.9091	98.105
3.2727	102.5
3.6364	106.9
4	111.3

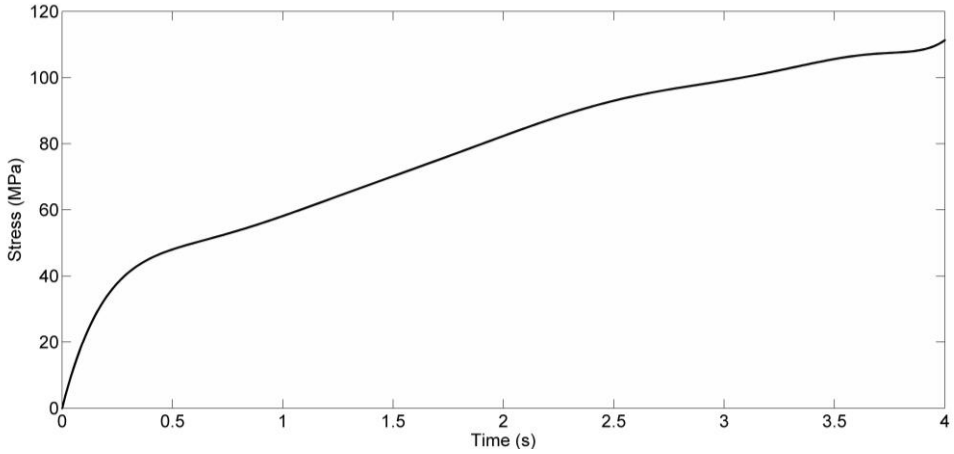

Figure 34: Stresses on baseplate in 4 seconds during shoulder joint flexion

4.1.3.2 Inferior Screw

The same result of Von Mises stress applied to the inferior screw for flexion movement in 4 seconds, shows that the maximum stress similarly happens at t= 4 Sec. at the end of the flexion range as shown in Figure 35. Maximum stresses distribution on inferior screw is presented in Table 16 and it is demonstrated as a plotted curve in Figure 36.

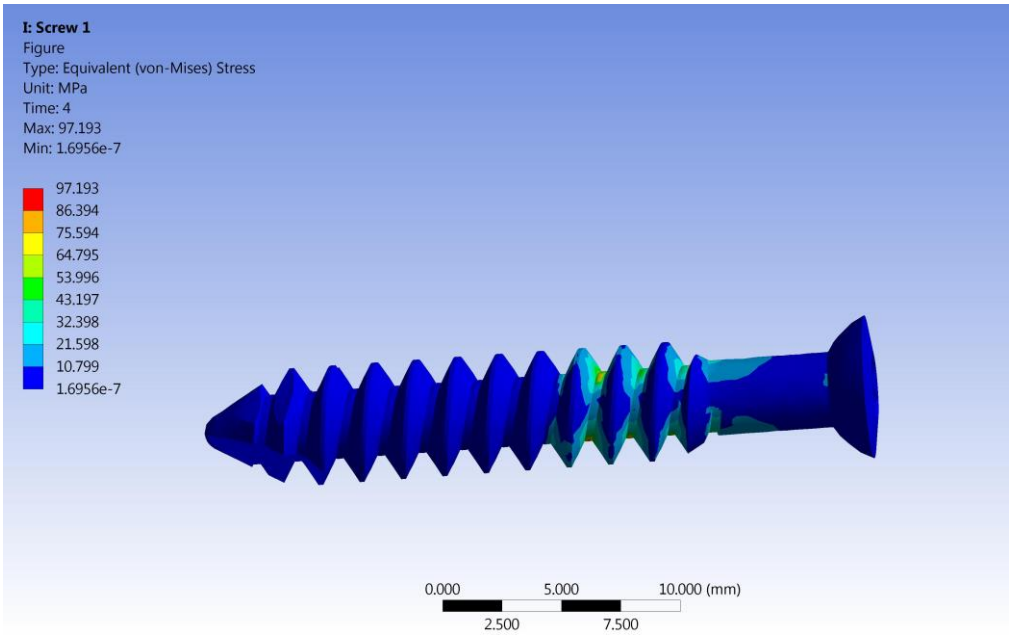

Figure 35: Maximum stress distribution on inferior screw during shoulder joint flexion at t=4 Sec.

Table 16: Stresses distribution on inferior screw during shoulder joint flexion in 4 seconds

Time (s)	Maximum stress (MPa)
0	0
0.36364	30.122
0.72727	38.154
1.0909	44.982
1.4545	48.195
1.8182	51.408
2.1818	59.44
2.5455	72.292
2.9091	85.144
3.2727	90.767
3.6364	93.98

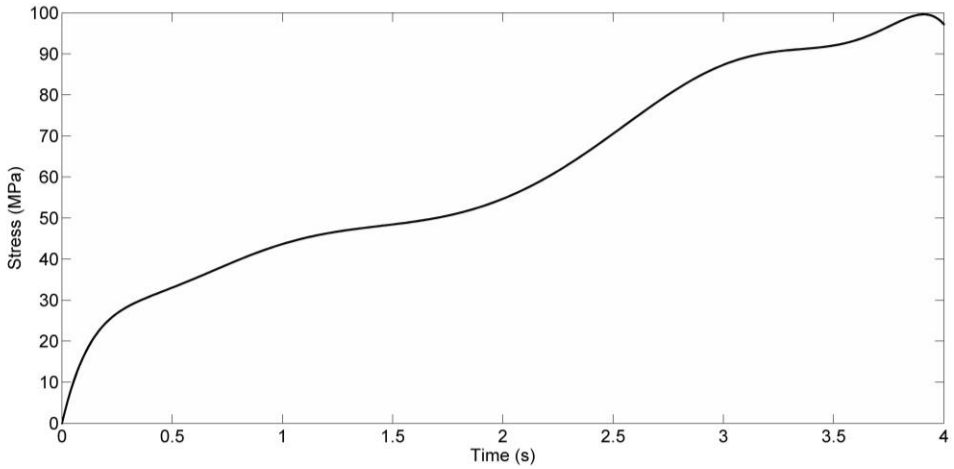

Figure 36: Stresses on inferior screw during shoulder joint flexion in 4 seconds

4.1.3.3 Superior Screw

Von Mises stress dispersal during shoulder flexion on superior screw in 4 seconds has the maximum stress at t= 3.63 Sec., which is also really close to the end of motion range and from the plotted figure it can be observed that this part`s stress is also in

direct correlation with time as the flexion angle increases as shown in Figure 37, Figure 38 and Table 17.

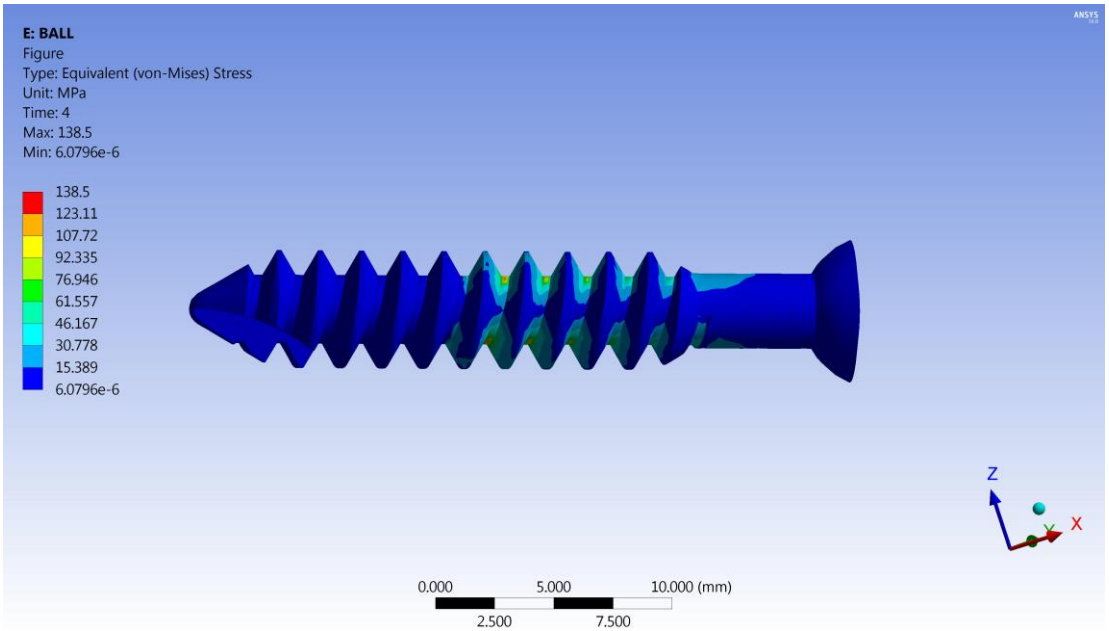

Figure 37: Maximum stress distribution on superior screw during shoulder joint flexion movement at t=4 Sec.

Table 17: Stresses distribution on superior screw during shoulder joint flexion movement in 4 seconds

Time (s)	Maximum stress (MPa)
0	0
0.36364	42.924
0.72727	54.371
1.0909	64.1
1.4545	68.679
1.8182	73.257
2.1818	84.704
2.5455	103.02
2.9091	121.33
3.2727	129.35
3.6364	133.92

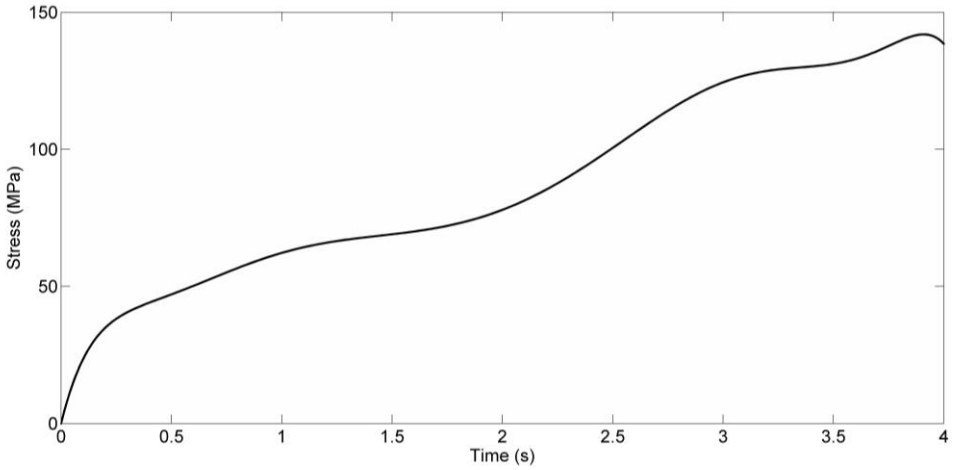

Figure 38: Stresses on superior screw during shoulder joint flexion movement in 4 seconds

4.1.3.4 Glenosphere

Following results are the Maximum Von Mises stress distribution on glenosphere during flexion movement of the shoulder implant in 4 seconds. The results shows that the maximum stress happens at end of motion at $t = 4$ Sec., and this result also shows that again the end of flexion motion is the most critical position inflexion. The stress distribution at the end of this motion can be observed in Figure 39. Maximum stresses distribution on glenosphere is presented in Table 18 and its curved plot is illustrated in Figure 40.

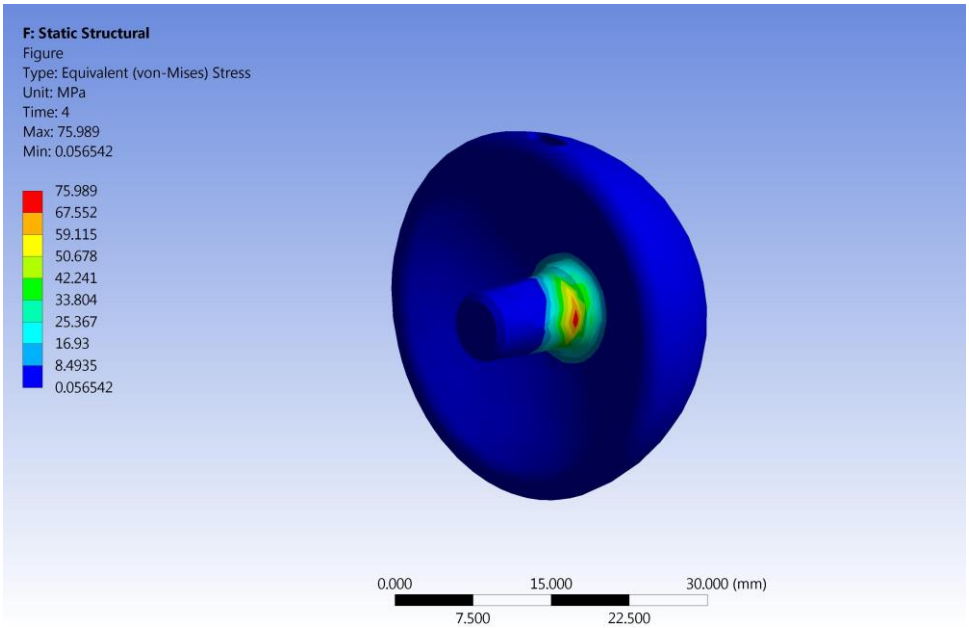

Figure 39: Maximum stress distribution on glenosphere during shoulder joint flexion movement at t=4 Sec.

Table 18: Stresses distribution on glenosphere during shoulder joint flexion movement in 4 seconds

Time (s)	Maximum stress (MPa)
0	0
0.36364	27.402
0.72727	30.928
1.0909	34.411
1.4545	37.879
1.8182	42.024
2.1818	45.094
2.5455	46.629
2.9091	48.165
3.2727	50.774
3.6364	58.719

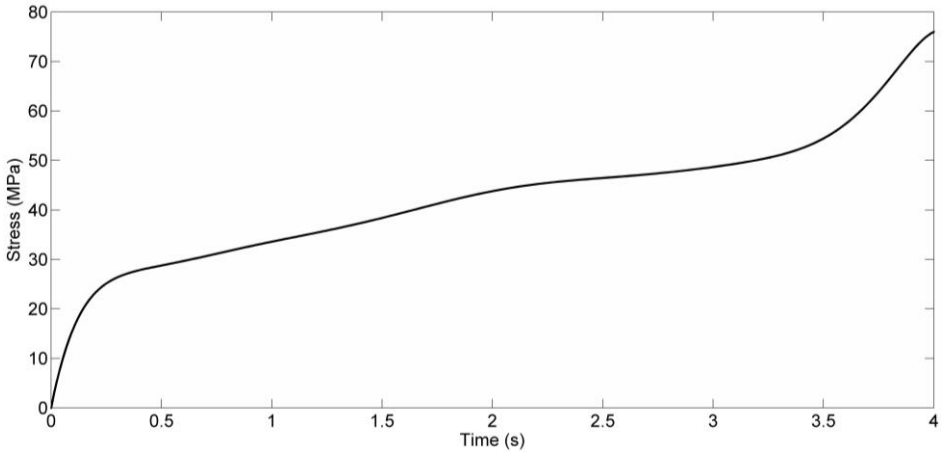

Figure 40: Stresses on glenosphere during shoulder joint flexion movement in 4 seconds

4.1.3.5 Humeral Cup

Similar results of Von Mises stress distribution on the humeral cup part of the implant during the 4 seconds flexion movement are as follow. The maximum Von Mises stress occurred at the end of flexion motion and the stress distribution at $t = 3.63$ Sec., is illustrated in Figure 41. Maximum stresses distribution in 4 seconds on humeral cup is presented in Table 19 and illustrated in Figure 42.

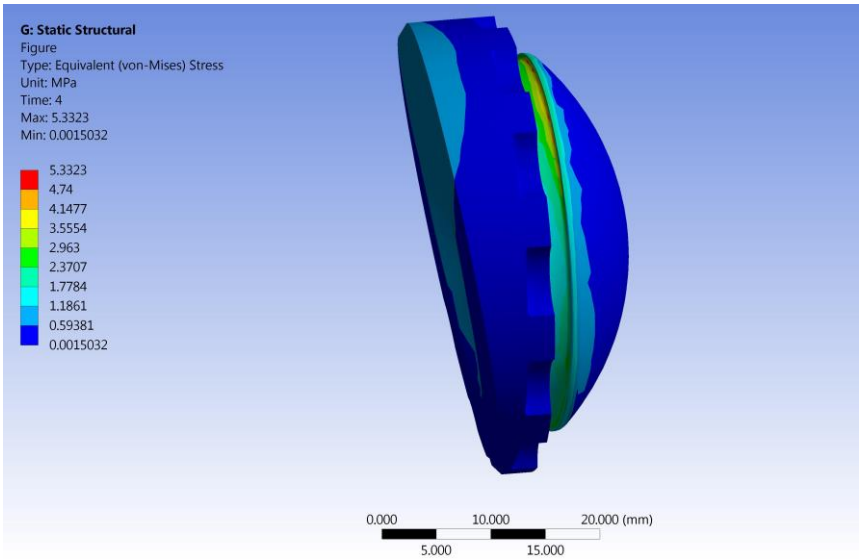

Figure 41: Maximum tress distribution on humeral cup during shoulder joint flexion movement at t=4 Sec.

Table 19: Stresses distribution on humeral cup during shoulder joint flexion movement in 4 seconds

Time (s)	Maximum stress (MPa)
0	0
0.36364	1.5081
0.72727	1.8528
1.0909	2.2406
1.4545	2.5207
1.8182	2.8654
2.1818	3.2963
2.5455	3.7703
2.9091	4.3089
3.2727	4.8044
3.6364	5.1168

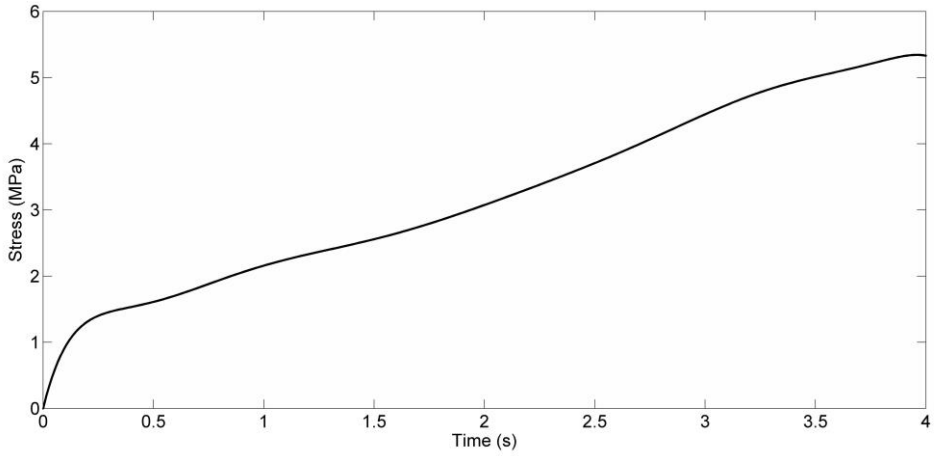

Figure 42: Stresses on humeral cup during shoulder joint flexion movement plotted in 4 seconds

4.1.3.6 Scapula

Similarly for the Scapula the results of Maximum Von Mises stress distribution during flexion movement in a 4 second time span is as follow. The maximum stress distribution happens again at the end of motion and in Figure 43 this distribution at $t = 3.63$ Sec., can be observed also because the stress increases as time passes.

Maximum stresses distribution on Scapula is presented in Table 20 and its plot is illustrated in Figure 44.

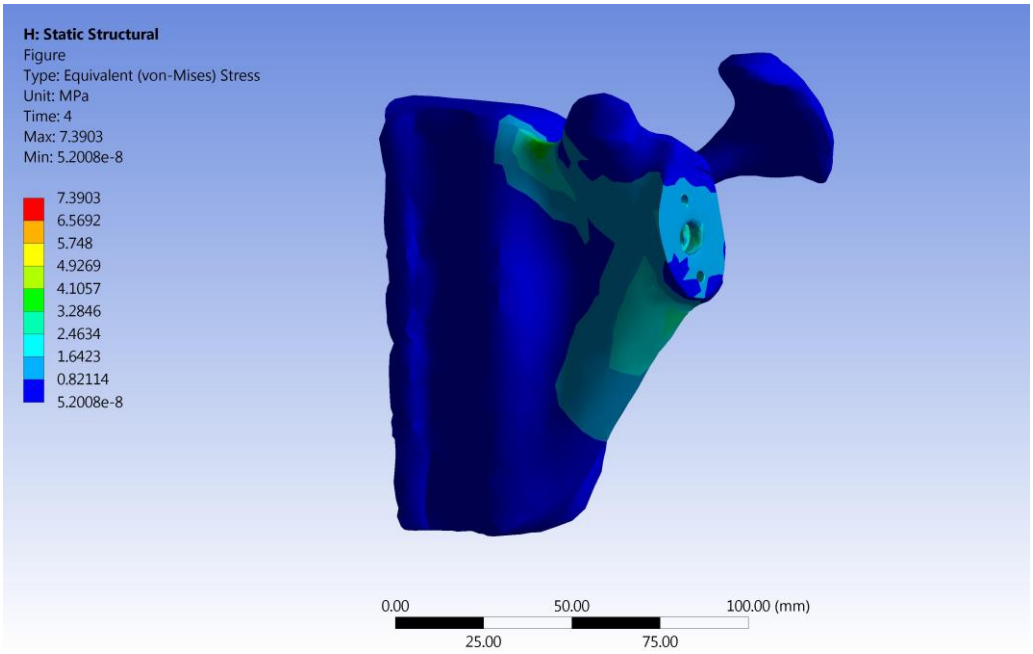

Figure 43: Maximum stresses distribution on scapula during shoulder joint rotation at t = 4 Sec.

Table 20: Stresses distribution on scapula during shoulder joint rotation in 4 seconds

Time (s)	Maximum stress (MPa)
0	0
0.36364	2.6874
0.72727	3.4398
1.0909	3.7623
1.4545	4.0311
1.8182	4.4611
2.1818	4.9985
2.5455	5.536
2.9091	6.0735
3.2727	6.611
3.6364	7.1216

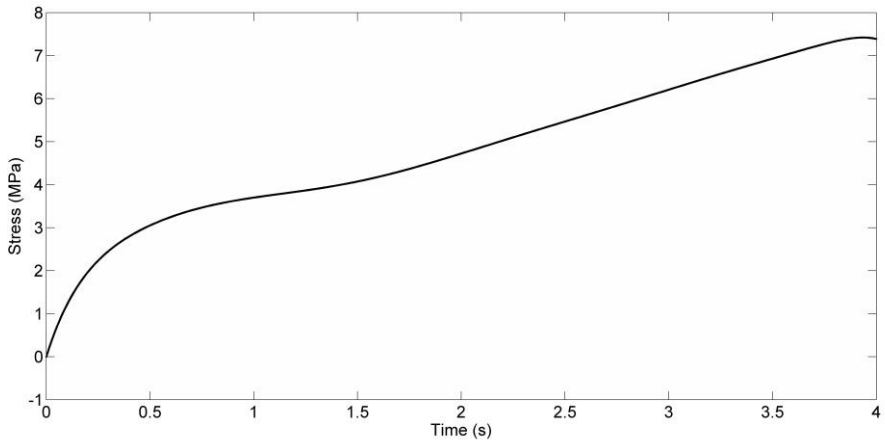

Figure 44: Stresses on scapula plot during shoulder joint flexion in 4 seconds

4.3 Comparison of Von Mises Stress on Implant Components during Abduction Rotation and Flexion Movements

After performing the Von Misses Stress analysis for reverse shoulder implant parts during some movements, it was found that at each movement the stresses change and affect the components in a different manner. In the following sections, the comparison of the presented results and results published previously are explained.

Chapter 5

DISCUSSION OF THE RESULTS

In this chapter the presented results in chapter 4 are evaluated and compared with similar studies.

As mentioned and illustrated previously, six different components of the reverse shoulder implant were designed through SolidWorks software and by the use of the ANSYS software it was analyzed for stress distribution by finite element method. The Von Mises stresses of each component were obtained in order to evaluate the stability of the shoulder implant and find out if a component would wear out or fail. The analysis was carried out three times for three different arm movements (abduction, rotation and flexion).

5.1 Stress Distribution Results during Abduction Movement

The Von Mises stress results during abduction for the baseplate, inferior and superior screws show that the maximum stress does not exceed the yield strength of the titanium alloy, so these parts would not yield or fail. According to these results the most critical component would be the inferior screw which has maximum Von Mises stress of 88 MPa, but since this value is approximately 10% of yield capacity of the titanium alloy (880 MPa), hence probability of any kind of failure in this component is very small. Similar results were obtained by Chebli et al [42] who analyzed the fixation of the glenoid component and in their study the critical component was also the inferior screw.

On the other hand the humeral cup maximum Von Mises stress is 26.46 MPa which exceeds yield strength of the polyethylene material. This would cause the component to wear or collapse during the abduction and this may also cause glenohumeral joint loosening which happens frequently according to the literature. These results are very close to the results of Swieszkowski et al. [43] who had obtained contact stress between humeral cup glenosphere during abduction movement and they obtained the stress value as 25.6 MPa. The difference between two results undoubtedly arises from the different assumption for analysis conditions. The possibility of wear happening at humeral cup is not high but the value is very close to compressive yield strength.

The glenosphere component itself has the maximum Von Mises stress of 87.12 MPa which does not exceed any of the material capacities of the CoCrMo (Cobalt-chrome or cobalt-chromium) alloy. So, this part does not become decisive in the design process. The material specifications of CoCrMo are presented in Chapter 3.

Overall assessment of the abduction results also shows that the almost in all of the shoulder components the stress increases as the time passes, and the maximum Von Mises stress appears at the end of the abduction movement. Except for the glenosphere component which its maximum Von Mises stress appears approximately in the middle of the movement.

5.2 Stress Distribution Results during Rotation Movement

The rotation results for the first three components; the baseplate, inferior screw and the superior screw, are very close to the abduction results with slightly less stress on the baseplate, making it less critical. However this time the critical screw becomes the superior screw which has the highest maximum Von Mises stress of 91 MPa. This

value is higher than the maximum stress of the inferior screw during abduction but again the stress value does not even reach 15% of the titanium alloy`s yield capacity (880 MPa). Hence even though this component in the implant has the highest stress level, it would not become a critical component for the design purposes.

The maximum stress for the humeral cup in the rotation movement is much smaller than the maximum stress appeared on this component during abduction and it is around 5 MPa. This small value indicates that in rotation movement the humeral cup does not become a critical part by exceeding its material capacities which is polyethylene.

Glenosphere component in rotation has a similar state as it had in abduction results, with even less maximum stress, which as explained in the abduction section, makes it even less critical among the components.

Also in rotation results, we can observe that the system bears the maximum stress at the middle of the movement according to the Von Mises stress results.

5.3 Stress Distribution Results during Flexion Movement

Results indicate that during the flexion movement, the maximum stress values for baseplate and two screws bear even more stress. The superior screw again becomes the critical component with the highest stress value by bearing almost 134 MPa stress output, which is higher than before but it is not still critical since is much smaller than titanium alloy`s capacity which is 880 MPa. So considering the results for all three movements the flexion movement appears to be the most important movement for the design of the titanium components of the implant. However the small ratios for the output stresses and the yield strength capacity of the titanium alloy suggests that these

titanium alloy components are suitable for the purposes of the reverse shoulder implant.

On the other hand during flexion the glenosphere and the humeral cup both show smaller stress value output than the abduction and even rotation, which makes flexion less decisive in the design of these two components.

Similar to abduction, in flexion the Von Mises stress of all the component even the glenosphere increases as the time passes and the maximum stress appears at the end of the movement for each component.

The summary of the results could be seen in the following Table 21.

Table 21: Comparison of stresses on implant components during abduction, rotation and flexion movements

Movements	**Highest Von Mises stress**	**Critical components**	**Maximum stress in the movement**
Abduction	Inferior screw	Humeral Cup	End of the movement
Rotation	Superior Screw	-	Middle of the movement
Flexion	Superior Screw	-	End of the movement

Chapter 6

CONCLUSION

As mentioned in the previous section the results of this study shows a promising success for further observations and improvement in component design. Generally the results suggest that almost all of the designed components under the aforementioned conditions could be trusted to perform in behalf of the normal healthy shoulder. However the humeral cup component which was made out of polyethylene, illustrated a slight weakness during abduction movement. This outcome surely calls for further research and development for the design of humeral cup.

Also the analysis itself as mentioned beforehand was considerably simplified in order to become applicable for our computers, hence more detailed and more accurate evaluation done by more advanced and powerful processing system would surely generate more reliable results.

This study evaluated the super positioned movements of the shoulder implant for abduction, rotation and flexion separately which are essential for the design, but in a further complex observation the system should be evaluated for combined translational and rotational movements as well. For example, human arm can (and usually does) rotate and abduct simultaneously which would lead to different and may be more critical stress output on the components. Hence making the analysis more immersive and more detailed would again lead to get more accurate and more reliable outputs.

Generally by removing any of the simplifications of the 3D model and the finite element analysis more beneficial results would be generated at the risk of more complex and more time consuming computing process.

This study could be considered an initiative research in evaluating today`s most usual approach for designing a reverse shoulder implant. Considering the great impact that the success or failure of this implant or any kind of other body implant may have on people`s life, this line of research should and already is considered as high priority studies in academia. Although so many other approaches are being studied and developed all around the world in order to address the biomechanical failures of the body, still this type of implantations are the most common ones and should be studied further more in depth.

REFERENCES

[1] Kronberg, M., Brostrom. L.A., Soderlund, V. (1990). Retroversion of the humeral head in the normal shoulder and its relationship to the normal range of motion. Clin Orthop.;253:113-117.

[2] Steinbruck, K. (1999) Epidemiology of sports injuries: 25-year analysis of sports orthopedic-traumatologic ambulatory care. *Sportverletz Sportschaden*.;13:38-52.

[3] Jobe, C.M. (1998). Gross anatomy of the shoulder. In: Rockwood C.A Jr, Matsen FA II, eds. The Shoulder. Vol 1. Philadelphia, PA: W.B Saunders;34-97.

[4] Rockwood, C.A Jr., Matsen F.A. HI, eds. (1998) The Shoulder. Vol 1. Philadelphia, P.A: WB Saunders;:233-263.

[5] Rockwood, C.A Jr., Williams, G.R., Young, DC. (1999) Injuries to the acromio-clavicular joint. In: Rockwood C.A Jr, Green D.P, Bucholz RW, eds.

[6] Hertz, H. (1984) Die bedeutung des limbus glenoidalis fur die stabilitat des schultergelenks. *Wein Klin Wochenschr Suppl*.;152:1-23.

[7] Rose, S.H., Melton, L.J., Monfey, B.F., Ilstrup, D.M., Riggs, L.B. (1982) Epidemiologic features of humeral fractures. *Clin Orthop*.;168:24-30.

[8] McCluskey, G.M. III, Todd, J. (1995) Acromioclavicular joint injuries. J South *Orthop Assoc*.206-213.

[9] Codman, E.A. (1934) The Shoulder, Rupture of the Supraspinatus Tendon and Other Lesions in or about the Subacromial Bursa. Boston, M.A: Thomas Todd.313-331.

[11] Hall, M.C., Rosser, M. (1963) The structure of the upper end of the humerus with reference to osteoporotic changes in senescence leading to fractures. *Can Medical Association* J.290-294.

[12] Wamer, J.J.P., Krushell, R.J., Masquelet, A., Gerber, C. (1992) Anatomy and relation-ships of the suprascapular nerve: anatomical constraints to mobilization of the supraspinatus and infraspinatus muscles in the management ofmassive rotator-cuff tears. J Bone Joint Surg Am.74:36-45.

[13] Ticker. J.B., Djurasovic, M., Strauch R.J. (1998) Incidence of ganglion cysts and other variations in anatomy along the course of the suprascapular nerve. J *Shoulder Elbow Surg*.7:472-478.

[14] Rockwood and Green's (1991) Fractures in Adults. Vol 1. 3rd ed. Philadelphia, P.A: JB Lippincott. 1181-1252.

[15] Astier, V., Thollon, L., Arnoux, P.J., Mouret, F. & Brunet, C., (2008). Development of a finite element model of the shoulder: application during a side impact. *International Journal of Crashworthiness*, 13(3): 301-312.

[16] M. Pandy. (2001) "Computer modelling and simulation of human movement". *Annual review of Biomehanical Engineering*, vol 3, pp 245-273.

[17] K. Hollerbach, A.M. Hollister, E. Ashby, "3-D Finite Element Model Development for Biomechanics: A Software Demonstration", *Sixth International Symposium on Computer Simulation Biomechanics*, Tokyo, Japan, 1997.

[18] Luo, Z.P., Hsu, H.C., Grabowski, J.J., Morrey, B.F. and An, K.N. (1998). Mechanical environment associated with rotator cuff tears. *Journal of Shoulder and Elbow Surgery*, 7(6): 616-620.

[19] P. Favre, J.G. Snedeker, C. Gerber. (2009) " Numerical modeling of the shoulder for clinical applications" Phil. Trans. R. Soc. A., vol. 367, pp. 2095–2118

[20] Torchia M.E, Cofield R.H. (1994) Long-term results of Neer total shoulder arthroplasty. Presented at: *The Tenth Open Meeting of the American Shoulder and Elbow Surgeons; New Orleans, Louisiana*.

[21] Sperling J.W., Cofield R.H., Rowland C. (1998): Neer hemiarthroplasty and Neer total shoulder arthroplasty in patients 50 years old or less. J Bone Joint Surg.;80A:464-73.

[22] Burkhead W.Z., Hutton K.S. (1995) Biologic resurfacing of the glenoid with hemiarthroplasty of the shoulder. *JShoulder Elbow Surg*. 4:263-270.

[23] Beredjiklian P.K., Iannotti J.P., Norris T.R., Williams GR. (1998) Operative treatment of malunion of a fracture of the proximal aspect of the humerus. J Bone Joint Surg. 80:1484-97.

[24] Wilber M.C., Evans E.B. (1997) Fractures of the scapula. An analysis of forty cases and a review of literature. J Bone Joint Surg Am 59: 358-62.

[25] Thompson D.A., Flynn T.C., Miller P.W., Fischer RP. (1985) The significance of scapular fractures. J Trauma 25:974-7.

[26] Veehof MM., Sleegers EJ., van Veldhoven N.H., Schuurman AH., van Meeteren NL. (2002) Psychometric qualities of the Dutch language version of the Disability of the Arm, *Shoulder and Hand questionnaire (DASH- DLV). J Hand Ther*;15:347-54.

[27] Ong K.L., Mowat FS., Chan N., Lau E., Halpern M.T., Kurtz S.M. (1995) Economic burden of revision hip and knee arthroplasty in Medicare enrollees.

[28] Sajadi K.R., Kwon Y.W., Zuckerman J.D. (2010) Revision shoulder arthroplasty: an analysis of indications and outcomes. *J Shoulder Elbow Surg* 2010.

[29] Cil A., Veillette C.J., Sanchez-Sotelo J., Sperling J.W., Schleck C., Cofield RH. (2009) Revision of the humeral component for aseptic loosening in arthroplasty of the shoulder. *J Bone Joint Surg* Br 91:75-81

[30] Dines J.S., Fealy S., Strauss E.J., Allen A., Craig E.V., Warren R.F., Dines D.M. (2006) Outcomes analysis of revision total shoulder replacement. *J Bone Joint Surg*. 88:1494-500.

[31] Bankes M.J., Emery R.J. (1995) Pioneers of shoulder replacement: Themistocles Gluck and Jules Emile Pean. *J Shoulder Elbow Surg*. 4:259–262.

[32] Emery R.J., Bankes M.J. (1999) Shoulder replacement: historical perspectives. In: Walch G., Boileau P., eds. *Shoulder Arthroplasty. Berlin, Germany: Springer*: 3–9.

[33] Martin T.G., Iannotti J.P. (2008) Reverse total shoulder arthroplasty for acute fractures and failed management after proximal humeral fractures. *Orthop Clin North Am.* 39:451-7

[34] De Wilde L.F., Plasschaert F.S., Audenaert E.A., Verdonk R.C. (2005) Functional recovery after a reverse prosthesis for reconstruction of the proximal humerus in tumor surgery. *Clin Orthop Relat Res*. 430:156-62.

[35] Anglin C. (1999) Shoulder prosthesis testing. PhD thesis. *Kingston: Queen's University*.

[36] Anglin C., Wyss U.P., Pichora D.R.(2000) Glenohumeral contact forces. Proc Inst Mech Eng [H]. In Press.

[37] De Wilde L., Mombert M., Van Petegem P., Verdonk R. (2001) Revision of shoulder replacement with a reversed shoulder prosthesis (Delta III): report of five cases. Acta Orthop Belg 67:348-53.

[38] Nyffeler R.W., Werner C.M., Simmen B.R., Gerber C. (2004) Analysis of a retrieved delta III total shoulder prosthesis. *J Bone Joint Surg Br* 86:1187-91.

[39] Simovitch R., Zumstein M., Lohri E., Helmy M., Gerber C. (2007) Predictors of scapular notching in patients managed with the Delta III reverse shoulder replacement. *J Bone Joint Surg Am*. 89:588–600.

[40] Rittmeister M., Kerschbaumer F. (2001) Grammont total shoulder arthroplasty in patients with rheumatoid arthritis and nonreconstructible rotator cuff lesions. *J Shoulder Elbow Surg*. 10:17–22.

[41] Sirveaux F., Favard L., Oudet D., et al. (2004) Grammont inverted total shoulder arthroplasty in the treatment of glenohumeral osteo- arthritis with massive cuff rupture of the cuff. Results of a multicenter study of 80 shoulders. *J Bone Joint Surg Br* 86:388-95.

[42] Chebli, C., Huber, P., Watling, J., Bertelsen, A., Bicknell, R. T., & Matsen, F. (2008). Factors affecting fixation of the glenoid component of a reverse total shoulder prothesis. *Journal of Shoulder and Elbow Surgery*, 17(2), 323-327.

[43] Swieszkowski, W., Piotr Bednarz, and P. J. Prendergast. (2003) "Contact stresses in the glenoid component in total shoulder arthroplasty." *Proceedings of the*

Institution of Mechanical Engineers, Part H: Journal of Engineering in Medicine 217.1: 49-57.

[44] Soboyejo, W. (2002). Mechanical Properties of Engineered Materials: CRC Press.

APPENDICES

Appendix 1. Glenospher Dimensions

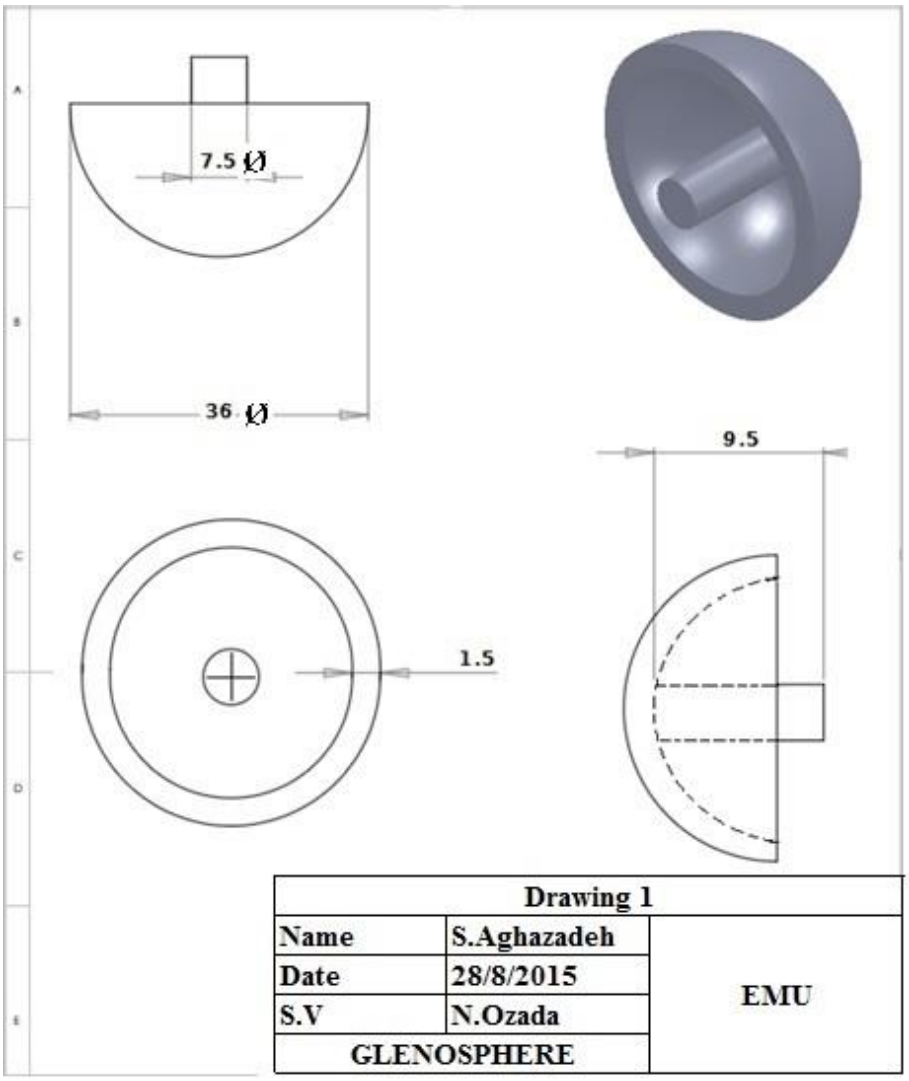

Drawing 1		
Name	S.Aghazadeh	EMU
Date	28/8/2015	
S.V	N.Ozada	
GLENOSPHERE		

Appendix 2. Baseplate Dimensions

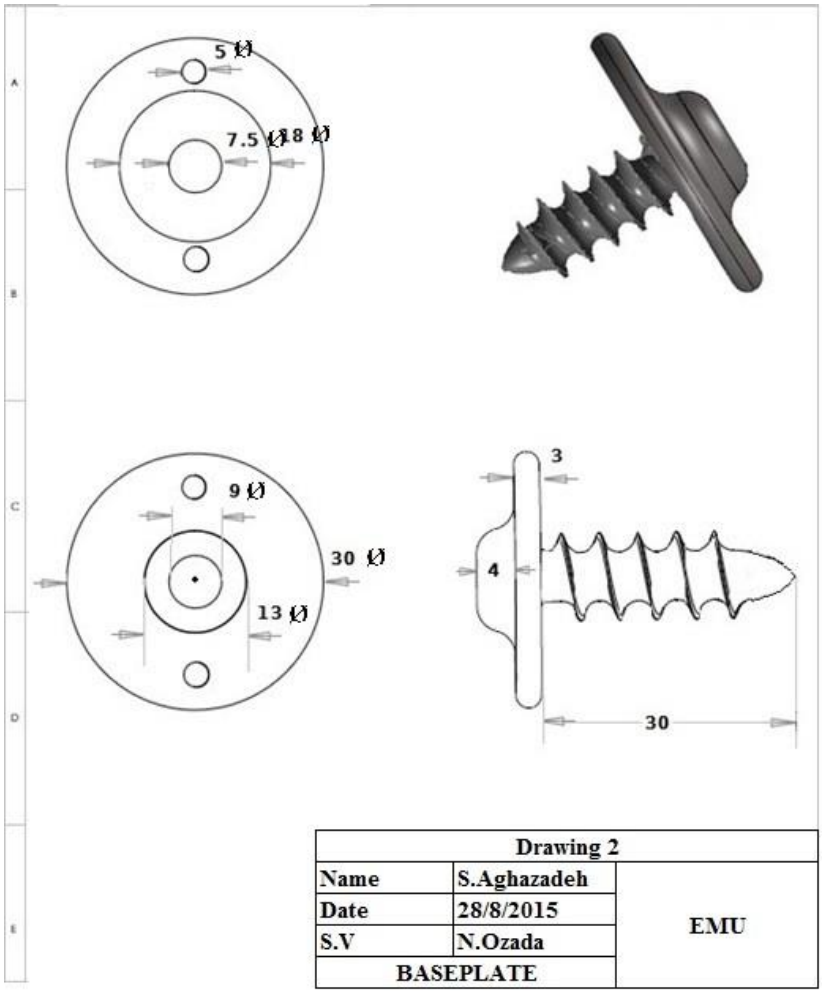

Drawing 2		
Name	S.Aghazadeh	EMU
Date	28/8/2015	
S.V	N.Ozada	
BASEPLATE		

Appendix 3. Humeral Cup Dimensions

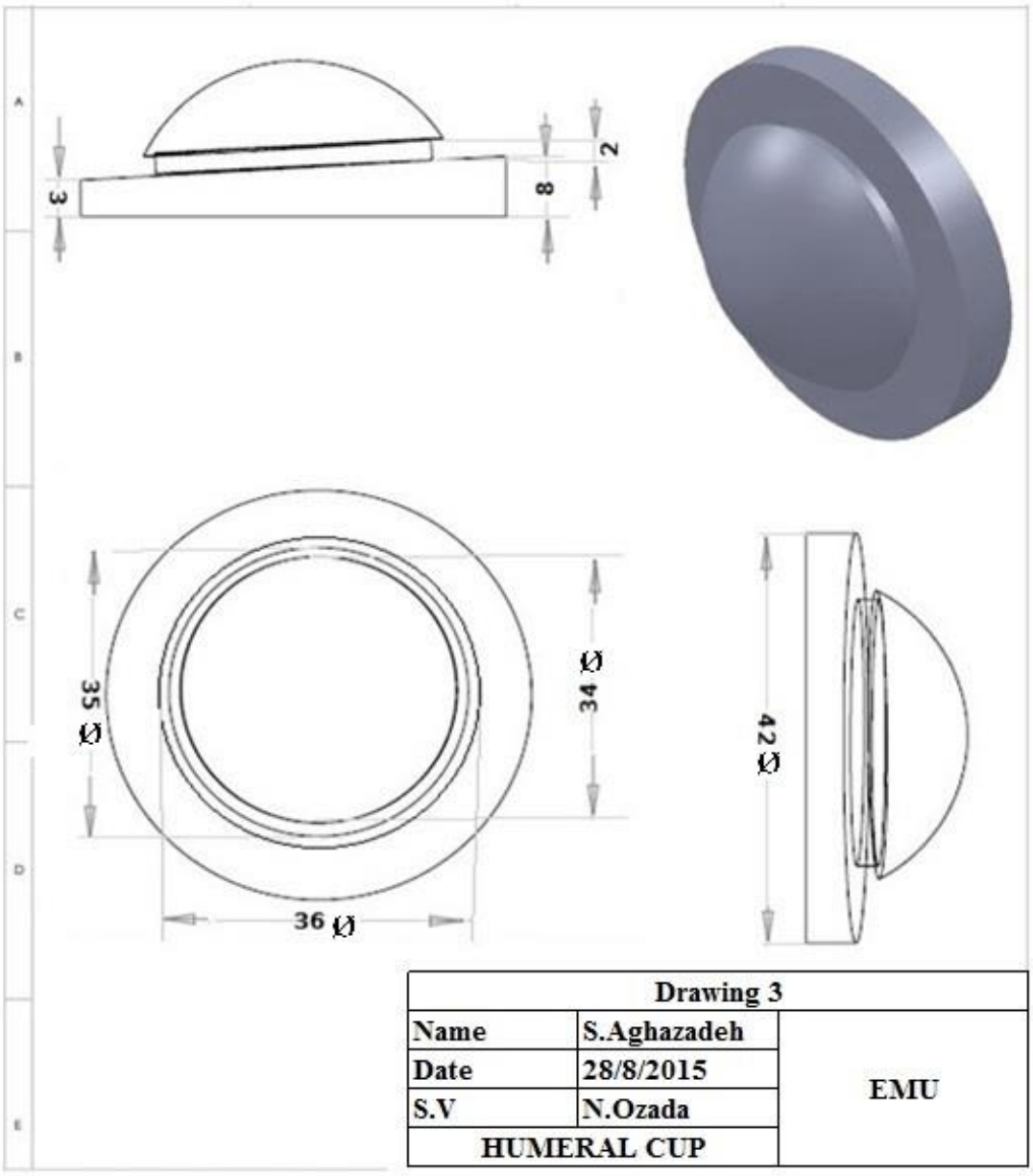

Drawing 3		
Name	S.Aghazadeh	EMU
Date	28/8/2015	
S.V	N.Ozada	
HUMERAL CUP		

Appendix 4. Humeral Stem

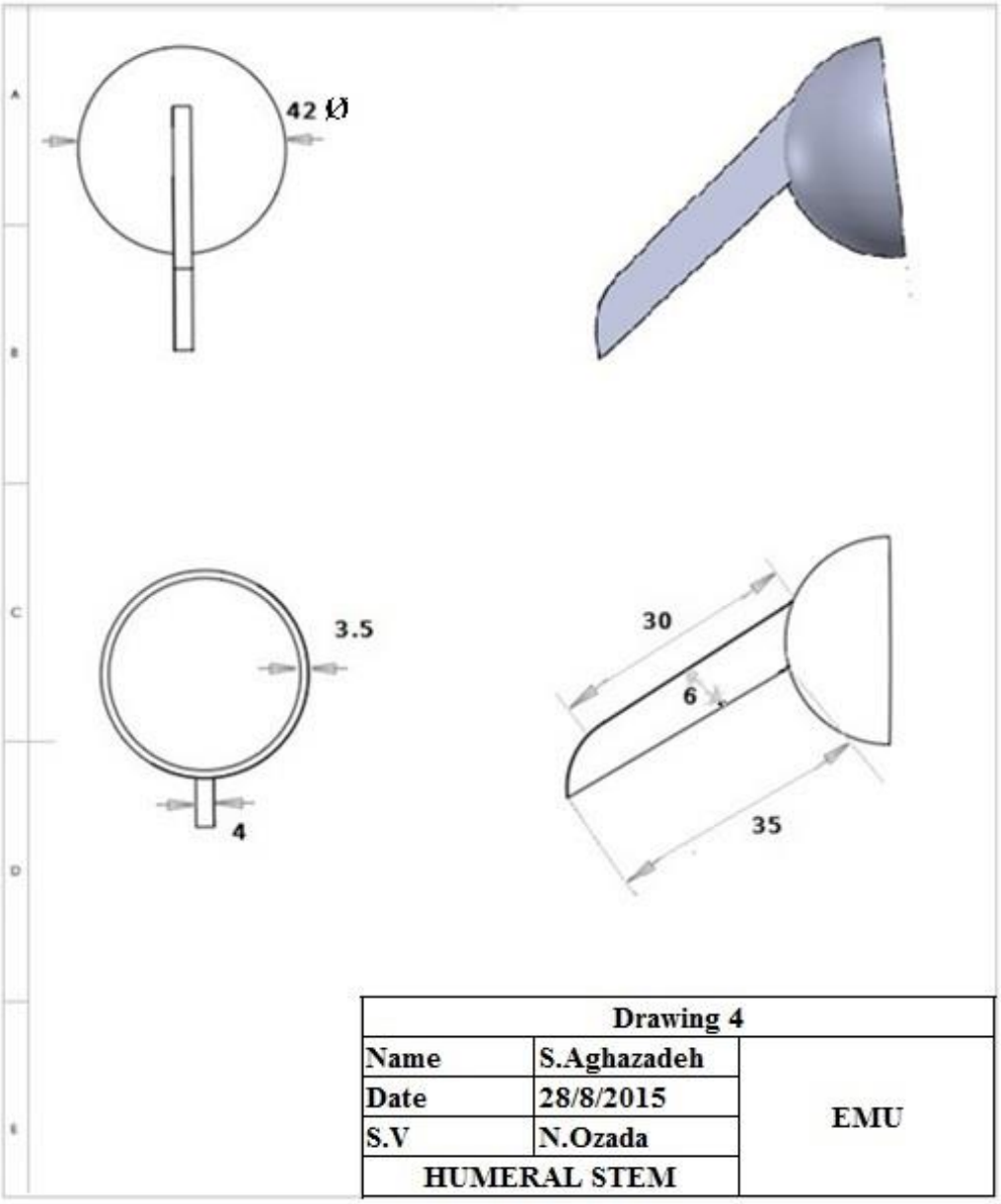

Drawing 4		
Name	S.Aghazadeh	EMU
Date	28/8/2015	
S.V	N.Ozada	
HUMERAL STEM		

Appendix 5. Inferior and Superior Screw Dimensions

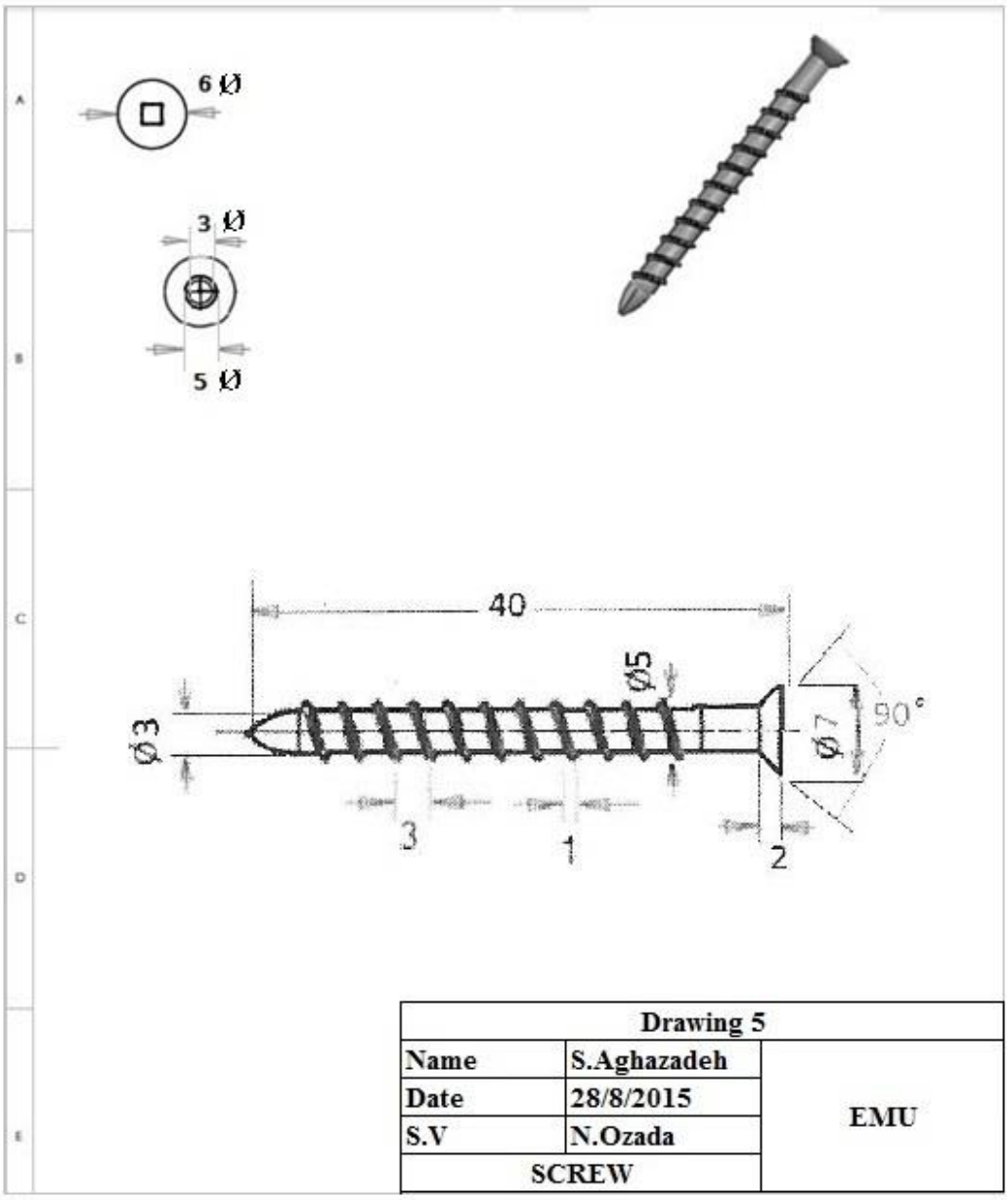

Drawing 5		
Name	S.Aghazadeh	EMU
Date	28/8/2015	
S.V	N.Ozada	
SCREW		